Table 2
Demographic characteristics and the results of SLR in patients with a localized lesion of the cerebellum

Case No.	Diagnosis	Age at examination	Age at onset	Sex	Lesion	Cerebellar ataxia		SLR			ABR
						Trunk	Lower limb (R/L)	Threshold (%)	Lying	Standing	
10	AVM	57	34	M	Lt. cerebellar hemisphere	−3	N/−2	>75	N/N	A/A	N.D.
11	AVM	33	32	M	Lt. cerebellum small	N	N/N	55	N/N	N/N	N
12	Infarct	77	75	F	Rt. cerebellar hemisphere + lacunas	−2	−1/N	65	N/N	A/N	N

Ataxia: mild (−0.5 to −1), moderate (−2 to −3), severe (−4); R, right; L, left; N, normal; A, absent; N.D., not done.
ABR, auditory brainstem response.

2.3. Experimental procedures

Each subject was asked to lie in a supine position and to keep the ankles dorsiflexed to about 20% of the maximum TA contraction while the SLR threshold was determined based on our previous study (Suga et al., 2001). When the SLR threshold was determined, we did not use stimulus intensities more than 75% of the maximum output of the stimulating device to ensure subject comfort. Next, magnetic cortical stimulations were performed using an intensity of 10% of the maximum stimulator output above the SLR threshold in the lying and standing positions to obtain the SPR and SLR (Sammut et al., 1995; Suga et al., 2001). Thus the maximum intensity used to elicit the SLR in a patient was 85% of the maximum stimulator output. We measured the latency and amplitude of the SPR and SLR in the lying and standing positions with a 20% TA voluntary contraction (standing on the heels). The SLR was defined as abnormal when it was absent, or when the latency of SLR exceeded the mean latency plus three standard deviations (SD) of the normal control. The SPR and primary TA responses were also defined as abnormal when the latency exceeded the mean latency plus three SD of the normal control.

2.4. Data analysis

The Wilcoxon signed rank test was used to compare the latencies and amplitudes of the SPR and SLR, between lying and standing positions. The Mann–Whitney *U*-test was used for the analysis of differences in latencies, amplitudes and amplitude ratios of the SPR and SLR, in supine and standing postures between patients and healthy controls. A p-value < 0.05 was considered to be statistically significant.

3. Results

The clinical findings of patients with cerebellar degeneration and the results of SPR and SLR data in the controls

Table 3
SLR and SPR data in normal controls and cerebellar degeneration patients

		Controls ($n = 11$)	Patients ($n = 9$)
SPR amplitude (mV)	Supine	0.34 ± 0.13	0.31 ± 0.15
	Standing	0.56 ± 0.37 **	0.73 ± 0.44 **
		*	
	Standing/supine	1.7 ± 1.1	2.8 ± 2.1
SPR latency (ms)	Supine	25.9 ± 3.0	28.5 ± 2.6
		**	
	Standing	25.0 ± 3.4	28.1 ± 2.2
		**	
SLR amplitude (mV)	Supine	0.55 ± 0.59	0.47 ± 0.36 ($n = 6$)
	Standing	0.41 ± 0.61 **	0.23 ± 0.15 ($n = 2$)
	Standing/supine	0.74 ± 0.4	0.46 ($n = 2$)
SLR latency (ms)	Supine	88.0 ± 8.1	88.1 ± 4.5 ($n = 6$)
	Standing	86.2 ± 7.2	98.9 ± 19.0 ($n = 2$)
TA amplitude (mV)	Supine	2.00 ± 1.0	1.96 ± 1.1
	Standing	2.23 ± 1.0	1.94 ± 0.95
TA latency (ms)	Supine	25.7 ± 2.4	25.9 ± 3.7
	Standing	25.6 ± 2.6	26.7 ± 2.7

Values are means ± SD.
*$p < 0.05$.
**$p < 0.01$.

and patients are shown in Tables 1 and 3. The mean ages of controls and patients with cerebellar degeneration were 52.3 and 57.9 years, respectively; their mean heights were 160 and 161 cm, respectively. These differences were not significant. MRI scans showed mild to severe cerebellar atrophy without brainstem atrophy in all patients.

Representative examples of SPR and SLR while lying and standing are shown in Fig. 1. Overall, an SPR was elicited in all patients, whether in a lying or standing position. SLRs were abnormal in patients, depending on the posture. The SLR threshold was higher than 75% of the maximum stimulator output in 3 out of 9 patients (Table 1), while no control subject showed an SLR threshold that was more than 75% of the maximum stimulator output ($62.3 \pm 5.6\%$, mean $\pm$ SD).

The SPR amplitudes of both controls and patients were significantly greater in a standing than in a lying position ($p < 0.01$). The SPR amplitudes were not significantly different between controls and patients, in either a standing or lying position (Table 3). However, the amplitude ratio of standing to lying position was significantly greater in patients than in controls ($p < 0.05$). In addition, the SPR latency of patients was significantly longer than that of controls in both conditions ($p < 0.01$), but did not exceed more than the mean control latency + 2 SD.

In normal controls, the SLR was easily elicited in all limbs in both lying and standing positions, and the amplitude of the SLR was significantly smaller in standing than in a lying position ($p < 0.01$). On the other hand, the SLR was absent from 4 patients in the lying position (or 7 of 18 limbs, 38.9%), while 8 patients (or 15 of 18 limbs, 83.3%) showed abnormal SLR in the standing position (Table 1). The amplitude and latency of the primary TA response were not significantly different between controls and patients, in either a supine or standing position (Table 3).

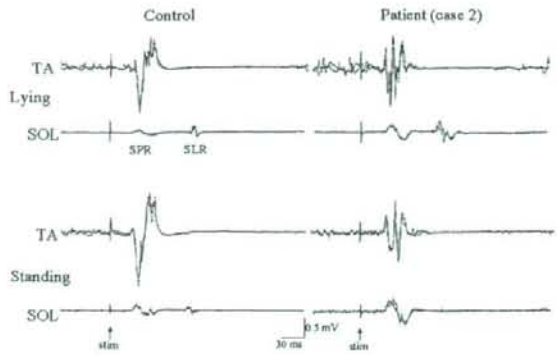

Fig. 1. Representative SPRs, SLRs and primary TA responses while lying (upper traces) and standing (lower traces). Two single trials are superimposed in each condition. The SLR is elicited in both lying and standing positions in a control subject (left). By contrast, it is obtained in the lying position, but not in the standing position, in a patient with cerebellar degeneration (right).

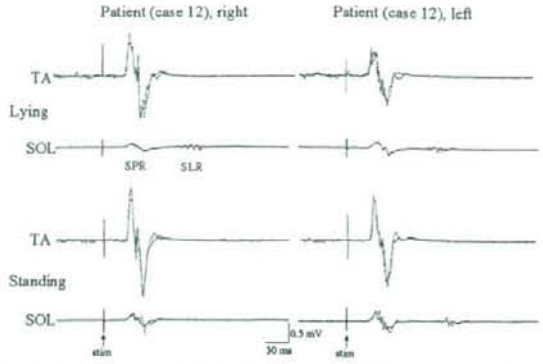

Fig. 2. Representative SPRs, SLRs and primary TA responses while lying (upper traces) and standing (lower traces) from Case 12. Two single trials are superimposed in each condition. The SLR is obtained in both sides in the lying position but not in right side (left) in the standing position.

The results in patients with localized cerebellar lesions defined by MRI are summarized in Table 2 (cases 10–12). Case 10 was a patient with AVM and a concomitant aneurysm. He was operated on when he was 34 years old. He later underwent γ-knife therapy at the age of 56. He showed moderate truncal and left lower limb ataxia at the time of the examination. The SLR threshold in this patient was more than 75% of the maximum stimulator output. The SLR of this patient was within the normal range in the lying position, but an SLR could not be elicited on either side when the patient was in the standing position. Case 11 was also a patient with AVM, and this

Fig. 3. T2 weighted MRI of Case 12. Right cerebellar infarctions with small pontine lesions are shown.

patient received γ-knife therapy at the age of 32. His only symptom then was mild left upper limb ataxia. An SLR was normally elicited in this patient on both sides, in both lying and standing positions. Case 12 suffered right cerebellar infarctions at the age of 75. She showed moderate truncal and mild right lower limb ataxia at the time of the examination. An SLR could not be elicited in the right SOL of this patient when she was in the standing position (Fig. 2). Her MRI revealed lesions in the right cerebellum and several small pontine lesions (Fig. 3), but she did not show pyramidal or extrapyramidal signs clinically. Her auditory brainstem response was normal. The SPR latencies of all 3 patients were normal.

4. Discussion

The SPR latency was unexpectedly prolonged in our cerebellar degeneration patients without apparent pyramidal signs, but it did not exceed more than the mean control latency + 2 SD. There have been a few reports indicating that a minority of patients with SCA 6 show extracerebellar signs, including pyramidal tract signs (Frontali, 2001; Geschwind et al., 1997; Gomez et al., 1997; Matsumura et al., 1997; Schöls et al., 1997; Takahashi et al., 2004). In TMS studies, the CMCT has been found to be either prolonged (Chen et al., 2004; Lee et al., 2003) or normal (Sakuma et al., 2005; Schwenkreis et al., 2002) in SCA 6. Lee et al. (2003) also reported that cortical relay time of the long latency reflex was prolonged in SCA 6 patients, and suggested that SCA 6 patients had dysfunctions of the transcortical polysynaptic pathways from the sensory to the motor cortices. In this study, the amplitudes and latencies of the primary TA responses were not significantly different between controls and patients in either a supine or standing position. This finding and the slight increase in SPR latency in ataxic patients suggest a subclinical dysfunction of the pyramidal tract or motor cortex in cases of cerebellar degeneration. What is the cause of the pyramidal tract dysfunction in 'pure' cerebellar ataxia? Sakuma et al. (2005) assumed that the reverse of crossed cerebellar diaschisis could be responsible for this phenomenon. Crossed cerebellar diaschisis is a matched depression of blood flow and metabolism in the cerebellar hemisphere contralateral to a focal cerebral lesion. Similarly, subsequent hypoperfusion is detected in the cerebral hemisphere contralateral to the cerebellar lesion in cases of crossed cerebello-cerebral diaschisis (Broich et al., 1987; Komaba et al., 2000). The dysfunction of the cerebellofugal pathway to the primary motor cortex may result in pyramidal tract dysfunction, which might cause the prolonged SPR latency we observed.

The results of our previous study (Suga et al., 2001) suggested that cerebellar function could influence the generation of the SLR, although a contribution from the extracerebellar system could not be fully excluded. In the present study, the SLR threshold of 3 patients with 'pure' cerebellar degeneration exceeded more than 75% of the maximum stimulator output. Similarly, one patient with a localized cerebellar lesion showed an elevated SLR threshold. The frequency of patients with an abnormal SLR was 38.9% in the lying position and 83.3% in the standing position. In addition, the results of the three patients with localized lesion of cerebellum showed that the severity of ataxia appeared to be related to the abnormal SLRs. From these results, we believe that the cerebellofugal system contributes significantly to the generation of SLRs. In accordance with this finding, we previously found that SLRs are normal in patients with ALS (Suga et al., 2001). This suggests that the SLR does not originate from the corticospinal tract. Sakihara et al. (2003) reported that repetitive TMS over the cerebellum evokes a small, late potential (about 100 ms latency and amplitude <50 μV) in the SOL in normal standing controls. They suggested that this late response was conducted from the cerebellum to the SOL via an as yet unknown descending pathway. Therefore, it is possible that the SLR elicited by TMS over the vertex and the late potential evoked by TMS over the cerebellum share a common pathway. Because evoking the SLR is a simple technique and is useful for pure cerebellar dysfunction, SLR could be a practical method to apply for evaluating cerebellar function.

The postural inhibition of SLR amplitude was significant in controls. In addition, the frequency of abnormal SLRs was markedly increased in ataxic patients standing on their heels. These results confirmed the effect of posture on SLR. Ertekin et al. (1995) reported that when the standing position was stable, the SLR was difficult to elicit. However, the SLR was enhanced when standing was made difficult in normal subjects. Therefore, SLR is closely related to postural control, which is significantly influenced by posture and cerebellar function.

The postural facilitation of SPR amplitude was small but significantly greater in patients with ataxia than in controls, quite opposite to the differences in SLR. Our previous study also showed that there was no significant correlation between the amplitudes of the SPR and SLR (Suga et al., 2001) in normal subjects. These findings support the idea that the mechanism for SLR generation is different from that for SPR generation. Ackermann et al. (1991) found a significant influence of posture on the amplitudes of SPR in healthy subjects. They inferred that the basic excitability of the motor neuron pool was enhanced while standing. However, the mechanisms for enhancing the SPR amplitude have not been fully explained. Our results suggest that the cerebellum also contributes to the postural facilitation of SPR. Ugawa et al. (1995) reported that a prior TMS over the cerebellum suppressed the MEPs of the hand muscle elicited by TMS over the contralateral motor cortex in normal subjects. However, this suppression effect was not elicited in patients with cerebellar dysfunction (Ugawa et al., 1995, 1997). Therefore, enhanced SPR related to postural change may reflect the degree of the inhibitory effect of the cerebellum on the motor cortex depending on the body posture.

In conclusion, abnormal SPR may reflect subclinical dysfunction of the corticospinal tract due to crossed cerebello-cerebral diaschisis. The SLRs were depressed in patients with SCA 6 and LCCA as well as in patients with localized cerebellar lesions compared with healthy subjects. This suggests that the cerebellum contributes significantly to the evoking of SLR in association with postural control. Therefore, both SPR and SLR can be useful parameters for evaluating 'pure' cerebellar function.

Acknowledgements

The authors thank Dr. Katsuya Ishido for recruiting some patients with a single cerebellar lesion. Part of this work was supported by grants for the Research Committee on rTMS treatment of movement disorders, the Ministry of Health and Welfare of Japan (17231401).

References

Ackermann H, Scholz E, Koehler W, Dichgans J. Influence of posture and voluntary background contraction upon compound muscle action potentials from anterior tibial and soleus muscle following transcranial magnetic stimulation. Electroencephalogr Clin Neurophysiol 1991;81:71–80.

Broich K, Hartmann A, Biersack HJ, Horn R. Crossed cerebello-cerebral diaschisis in a patient with cerebellar infarction. Neurosci Lett 1987;83:7–12.

Chen JT, Lin YY, Lee YC, Soong BW, Wu ZA, Liao KK. Prolonged central motor conduction time of lower limb muscle in spinocerebellar ataxia 6. J Clin Neurosci 2004;11:381–3.

Dimitrijević MR, Kofler M, McKay WB, Sherwood AM, Van der Linden C, Lissens MA. Early and late lower limb motor evoked potentials elicited by transcranial magnetic motor cortex stimulation. Electroencephalogr Clin Neurophysiol 1992;85:365–73.

Ertekin C, Ertaş M, Efendi H, Larsson LE, Şirin H, Araç N, et al. A stable late soleus EMG response elicited by cortical stimulation during voluntary ankle dorsiflexion. Electroencephalogr Clin Neurophysiol 1995;97:275–83.

Frontali M. Spinocerebellar ataxia type 6: channelopathy or glutamine repeat disorder? Brain Res Bull 2001;56:227–31.

Geschwind DH, Perlman S, Figueroa KP, Karrm J, Baloh RW, Pulst SM. Spinocerebellar ataxia type 6. Frequency of the mutation and genotype–phenotype correlations. Neurology 1997;49:1247–51.

Gomez CM, Thompson RM, Gammack JT, Perlman SL, Dobyns WB, Truwit CL, et al. Spinocerebellar ataxia type 6: gaze-evoked and vertical nystagmus, Purkinje cell degeneration, and variable age of onset. Ann Neurol 1997;42:933–50.

Holmes G. The croonian lectures on the clinical symptoms of cerebellar disease and their interpretation. Lancet 1922;200:59–65.

Holmgren H, Larsson LE, Pedersen S. Late muscular responses to transcranial cortical stimulation in man. Electroencephalogr Clin Neurophysiol 1990;75:161–72.

Komaba Y, Osono E, Kitamura S, Katayama Y. Crossed cerebellocerebral diaschisis in patients with cerebellar stroke. Acta Neurol Scand 2000;101:8–12.

Lavoie BA, Cody FWJ, Capaday C. Cortical control of human soleus muscle during volitional and postural activities studied using focal magnetic stimulation. Exp Brain Res 1995;103:97–107.

Lee YC, Chen JT, Liao KK, Wu ZA, Soong BW. Prolonged cortical relay time of long latency reflex and central motor conduction in patients with spinocerebellar ataxia type 6. Clin Neurophysiol 2003;114:458–62.

Matsumura R, Futamura N, Fujimoto Y, Yanagimoto S, Horikawa H, Suzumura A, et al. Spinocerebellar ataxia type 6. Molecular and clinical features of 35 Japanese patients including one homozygous for the CAG repeat expansion. Neurology 1997;49:1238–43.

Sakihara K, Yorifuji S, Ihara A, Izumi H, Kono K, Takahashi Y, et al. Transcranial magnetic stimulation over the cerebellum evokes late potential in the soleus muscle. Neurosci Res 2003;46:257–62.

Sakuma K, Adachi Y, Fukuda H, Kai T, Nakashima K. Triple stimulation technique in patients with spinocerebellar ataxia type 6. Clin Neurophysiol 2005;116:2586–91.

Sammut R, Thickbroom GW, Wilson SA, Mastaglia FL. The origin of the soleus late response evoked by magnetic stimulation of human motor cortex. Electroencephalogr Clin Neurophysiol 1995;97:164–8.

Schöls L, Amoiridis G, Büttner T, Przuntek H, Epplen JT, Riess O. Autosomal dominant cerebellar ataxia: phenotypic differences in genetically defined subtypes? Ann Neurol 1997;42:924–32.

Schwenkreis P, Tegenthoff M, Witscher K, Börnke C, Przuntek H, Malin JP, et al. Motor cortex activation by transcranial magnetic stimulation in ataxia patients depends on the genetic defect. Brain 2002;125:301–9.

Suga R, Tobimatsu S, Taniwaki T, Kira J, Kato M. The soleus late response elicited by transcranial magnetic stimulation reflects agonist-antagonist postural adjustment in the lower limbs. Clin Neurophysiol 2001;112:2300–11.

Takahashi H, Ishikawa K, Tsutsumi T, Fujigasaki H, Kawata A, Okiyama R, et al. A clinical and genetic study in a large cohort of patients with spinocerebellar ataxia type 6. J Hum Genet 2004;49:256–64.

Ugawa Y, Uesaka Y, Terao Y, Hanajima R, Kanazawa I. Magnetic stimulation over the cerebellum in humans. Ann Neurol 1995;37:703–13.

Ugawa Y, Terao Y, Hanajima R, Sakai K, Furubayashi T, Machii K, et al. Magnetic stimulation over the cerebellum in patients with ataxia. Electroencephalogr Clin Neurophysiol 1997;104:453–8.

Valls-Solé J, Alvarez R, Tolosa ES. Responses of the soleus muscle to transcranial magnetic stimulation. Electroencephalogr Clin Neurophysiol 1994;93:421–7.

Wochnik-Dyjas D, Glazowski C, Niewiadomska M. Peculiarity of soleus motor potentials evoked by transcranial magnetic stimulation and electrical stimulation of tibial nerve. Electroencephalogr Clin Neurophysiol 1998;109:369–75.

ELSEVIER

NeuroImage

www.elsevier.com/locate/ynimg
NeuroImage 36 (2007) 1263–1276

Age-related alterations of the functional interactions within the basal ganglia and cerebellar motor loops *in vivo*

Takayuki Taniwaki,[a,b,d,*] Akira Okayama,[a] Takashi Yoshiura,[c] Osamu Togao,[c] Yasuhiko Nakamura,[c] Takao Yamasaki,[b] Katsuya Ogata,[b] Hiroshi Shigeto,[a] Yasumasa Ohyagi,[a] Jun-ichi Kira,[a] and Shozo Tobimatsu[b]

[a]*Department of Neurology, Graduate School of Medical Sciences, Kyushu University, Maidashi 3-1-1, Fukuoka 812-8582, Fukuoka, Japan*
[b]*Department of Clinical Neurophysiology, Neurological Institute, Graduate School of Medical Sciences, Kyushu University, Maidashi 3-1-1, Fukuoka 812-8582, Fukuoka, Japan*
[c]*Department of Clinical Radiology, Graduate School of Medical Sciences, Kyushu University, Maidashi 3-1-1, Fukuoka 812-8582, Fukuoka, Japan*
[d]*Division of Respirology, Neurology and Rheumatology, Department of Medicine, Kurume University School of Medicine, Asahi-machi 67, Kurume, Fukuoka 830-0011, Fukuoka, Japan*

Received 30 November 2006; revised 29 March 2007; accepted 2 April 2007
Available online 25 April 2007

Aging may alter the motor functions of the basal ganglia and cerebellum; however, no previous neuroimaging study has investigated the effect of aging on the functional connectivity of the motor loops involving these structures. Recently, using fMRI with a parametric approach and structural equation modeling (SEM), we demonstrated a significant functional interaction within the basal ganglia–thalamo–motor (BGTM) loop during self-initiated (SI) finger movement in young normal subjects, whereas cerebro–cerebellar (CC) loop was mainly involved during externally triggered (ET) movement. We applied this method to 12 normal aged subjects (53–72 years old) in order to study the effect of age on BGTM and CC loops. Compared with the functional connectivity seen in young subjects, SEM showed decreased connectivity in BGTM loops during SI task, decreased interaction in the CC loop during ET task, and increased connectivity within motor cortices and between hemispheres during both types of tasks. These results suggest an age-related decline of cortico-subcortical connectivity with increased interactions between motor cortices. Aging effects on SI and ET movements are probably caused by functional alterations within BGTM and CC loops.

Keywords: Aging; Basal ganglia; Cerebellum; Motor loop; fMRI; Structural equation modeling

Introduction

It is well documented that normal aging is associated with deterioration in cognitive (Grady, 2000; Hedden and Gabrieli, 2004; Mark and Rugg, 1998; Park et al., 2003) and motor functions (Calautti et al., 2001; Mattay et al., 2002; Sailer et al., 2000; Welford, 1988). In particular, slowing of motor movements and loss of fine motor skills are characteristic motor alterations of aging (Smith et al., 1999). The basal ganglia and cerebellum are two groups of subcortical nuclei that have been regarded as innate motor structures (Casini and Ivry, 1999; Ivry et al., 1988; Laforce and Doyon, 2002; O'Boyle et al., 1996; Pastor et al., 1992, 2004; Vakil et al., 2000), which might contribute to the motor alterations of aging. Studies of postmortem tissue have revealed a predominant decline with age in the motor systems of the basal ganglia (Kaasinen et al., 2000; Mann and Yates, 1979; Volkow et al., 1998) and the cerebellum (Andersen et al., 2003). However, functional brain imaging studies have shown greater activation not only in the striatum, thalamus and cerebellum but also in the supplementary motor area, sensorimotor cortex and ventral premotor cortex in normal aged subjects (Fang et al., 2005; Hutchinson et al., 2002; Mattay et al., 2002; Wu and Hallett, 2005; Ward and Frackowiak, 2003).

The connections of the basal ganglia and cerebellum are organized into discrete circuits or 'loops' that reciprocally interconnect a large and diverse set of cerebral cortical areas with the basal ganglia and cerebellum (Alexander et al., 1990; Middleton and Strick, 2000). From a functional point of view, the basal ganglia should not be viewed in isolation, but, rather, in the context of its connections to other brain areas within these loops (Alexander et al., 1990); the same consideration applies to the cerebellum. However, no study has investigated

Abbreviations: Put, putamen; GPi, internal segment of the globus pallidus; VL, ventrolateral nucleus of the thalamus; VPL, ventro–posterior–lateral nucleus of the thalamus; SMA, supplementary motor area; SMC, sensorimotor cortex; PMv, ventral premotor cortex; CB, cerebellar hemisphere (anterior lobe); DN, dentate nucleus of the cerebellum.

* Corresponding author. Division of Respirology, Neurology and Rheumatology, Department of Medicine, Kurume University School of Medicine, Fukuoka 830-0011, Japan.
E-mail address: ttaniwa@med.kurume-u.ac.jp (T. Taniwaki).
Available online on ScienceDirect (www.sciencedirect.com).

1053-8119/$ - see front matter © 2007 Elsevier Inc. All rights reserved.
doi:10.1016/j.neuroimage.2007.04.027

the effect of aging on the dynamic functional organization of the basal ganglia–thalamo–motor (BGTM) and cerebro-cerebellar (CC) loops *in vivo*. Recently, using fMRI combined with a parametric approach and structural equation modeling (SEM), we demonstrated functional interactions within the BGTM loop during self-initiated (SI) finger movement in normal young subjects, whereas the CC loop was involved during externally triggered (ET) movement (Taniwaki et al., 2003; 2006). The present study applies the same methods in order to investigate the effect of aging on the BGTM and CC loops *in vivo*. To achieve this, we compared functional network models of healthy young and old subjects.

Materials and methods

Participants

Twelve healthy aged subjects (mean age±SD, 62.9±7.0 years old; range, 53–72 years old; 7 men and 5 women) participated in the study. Data from 12 normal young subjects (mean age±SD, 24.9±1.5 years old; range, 23–29 years old; 9 men and 3 women) (Taniwaki et al., 2006) were used for comparison. The subjects were deemed healthy from their clinical histories, neurological examinations and normal blood pressure. No subjects were taking any medication that could affect brain excitability. For all subjects,

Table 1
Parametric analysis of rate-dependent BOLD effects *in young and aged subjects*

	Young subjects								Old subjects							
	Main effect				Linear effect				Main effect				Linear effect			
	Coordinates				Coordinates				Coordinates				Coordinates			
	Z	*x*	*y*	*z*	*Z*	*x*	*y*	*z*	*Z*	*x*	*y*	*z*	*Z*	*x*	*y*	*z*
SI movement																
rPut	5.25	30	−12	−2	4.03	28	−6	0	3.63	22	−8	2	n.s.			
rGPi	2.08	18	−6	−4	3.29	10	−2	−2	3.85	20	−2	2	n.s.			
rVL	4.48	10	−16	8	3.41	16	−14	16	4.31	14	−12	16	n.s.			
rVPL	4.54	14	−20	6	5.12	18	−22	6	3.14	12	−18	2	n.s.			
rSMA	4.42	4	0	50	3.86	6	−2	40	3.85	2	0	54	n.s.			
rSMC	6.09	36	−20	60	4.28	48	−20	52	4.86	40	−28	42	3.37	42	−12	54
rPMv	4.23	54	6	34	n.s.				3.72	58	4	34	3.50	40	−8	40
lCB	5.49	−28	−50	−28	n.s.				3.79	−24	−58	−24	2.92	−26	−74	−22
lDN	4.99	−14	−56	−22	n.s.				4.72	−12	−52	−18	n.s.			
lPut	n.s.				2.69	−26	−14	4	3.66	−22	0	2	n.s.			
lGPi	n.s.				2.94	−12	0	0	3.77	−14	0	4	n.s.			
lVL	3.97	−16	−8	12	n.s.				3.30	−14	−10	12	n.s.			
lVPL	4.21	−14	−16	6	3.24	−12	−20	8	4.83	−18	−20	12	4.23	−22	−18	12
lSMA	5.39	−2	−2	54	3.34	−6	0	42	4.73	−6	0	50	n.s.			
lSMC	4.49	−64	−18	34	4.29	−40	−18	58	4.75	−42	−30	40	3.21	−52	−16	48
lPMv	4.53	−58	4	38	2.73	−56	0	32	3.63	−54	8	42	3.19	−52	−8	38
rCB	4.25	26	−56	−26	4.08	26	−56	−26	4.47	28	−62	−26	n.s.			
rDN	4.21	22	−62	−24	4.48	18	−54	−22	4.18	20	−52	−24	3.52	20	−60	−26
ET movement																
rPut	3.91	30	−10	−2	n.s.				5.53	26	0	−2	n.s.			
rGPi	3.08	18	−6	−2	n.s.				4.27	18	−6	2	n.s.			
rVL	3.83	12	−18	0	n.s.				4.89	18	−16	14	n.s.			
rVPL	3.25	12	−22	8	3.44	16	−22	12	4.92	12	−20	8	n.s.			
rSMA	4.21	2	−2	54	n.s.				5.33	6	0	50	3.23	2	−4	48
rSMC	5.19	34	−14	56	3.82	46	−18	54	8.04	34	−16	56	2.89	48	−20	52
rPMv	3.58	54	2	34	2.99	52	2	38	5.24	56	4	32	2.70	52	−6	42
lCB	5.44	−32	−44	−30	3.94	−30	−54	−22	5.10	−30	−48	−26	3.88	−26	−68	−16
lDN	5.23	−20	−54	−22	3.92	−22	−50	−22	5.21	−12	−56	−24	3.30	−8	−54	−22
lPut	n.s.				n.s.				5.88	−26	−18	2	n.s.			
lGPi	n.s.				n.s.				n.s.				n.s.			
lVL	3.83	−18	−12	18	2.98	−12	−12	12	5.78	−12	−6	8	n.s.			
lVPL	3.09	−14	−18	6	n.s.				5.58	−10	−16	6	n.s.			
lSMA	3.40	−6	−2	44	n.s.				5.78	−6	0	48	n.s.			
lSMC	3.49	−64	−20	38	n.s.				5.43	−42	−8	54	3.38	−50	−12	44
lPMv	3.83	−56	−4	36	n.s.				3.94	−58	0	34	n.s.			
rCB	3.29	26	−66	−24	n.s.				4.84	34	−46	−28	3.23	36	−66	−18
rDN	4.13	22	−52	−22	n.s.				5.01	24	−50	−24	3.83	16	−52	−20

Z-values refer to activation maxima within the respective region, $p<0.001$ uncorrected, height threshold $Z>3.09$ or $p<0.01$ uncorrected, $Z>2.33$ in linear effect; SPM coordinates in parenthesis; n.s. = activation below height threshold, Put = putamen, GPi = internal segment of globus pallidus, VL = ventrolateral nucleus of thalamus, VPL = ventro–posterior–lateral nucleus of thalamus, SMA = supplementary motor area, SMC = sensorimotor cortex, PMv = ventral premotor cortex, CB = anterior lobe of the cerebellar hemisphere, DN = dentate nucleus of the cerebellum, r = right, l = left; in this and subsequent tables.

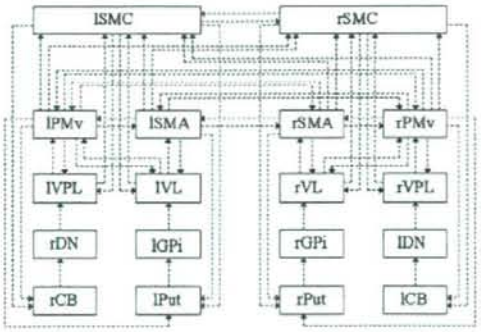

Fig. 1. A diagram illustrating the major cortical and subcortical structures involved in the sequential finger movements of SI and ET tasks, and their interconnections. These structures are organized into a basal ganglia–thalamo–motor loop, a cerebello-cerebral loop and connectivity within motor cortices. *Abbreviations:* Put, putamen; GPi, internal segment of the globus pallidus; VL, ventrolateral nucleus of the thalamus; VPL, ventro-posterior-lateral nucleus and X area of the thalamus; SMA, supplementary motor area; SMC, primary sensory-motor cortex; PMv, ventral premotor cortex; CB, cerebellar hemisphere (anterior lobe); DN, dentate nucleus of the cerebellum. r = right, l = left in this and subsequent figures.

no significant pathological change was found by anatomical T1- and T2-weighted MRI, although there were some changes due to normal aging. All subjects were strongly right-handed as assessed by a modified version of the Edinburgh handedness inventory (Oldfield, 1971). Informed written consent was obtained from all subjects for participation in this study. The local ethical committee of Kyushu University approved this study.

Experimental design

The activation paradigm consisted of sequential movements performed with the left hand as previously described (Taniwaki et al., 2003; 2006). We intended to reveal the movement-rate-related activity but not simple repetitive or externally cued movements. From our previous study (Taniwaki et al., 2003; 2006), sequential or internally cued movement could indicate movement-rate-related activity of the basal ganglia. Non-dominant hand movements cause a greater recruitment of the striatum (Mattay et al., 1998) and cerebellum (Jancke et al., 1999). Thus, we used sequential finger movements in the left hand.

Subjects were instructed to move each finger with changing movement rates. They were then required to practice the tasks before they were scanned, until they were able to perform them at constant amplitude without error. They were also instructed to keep their eyes

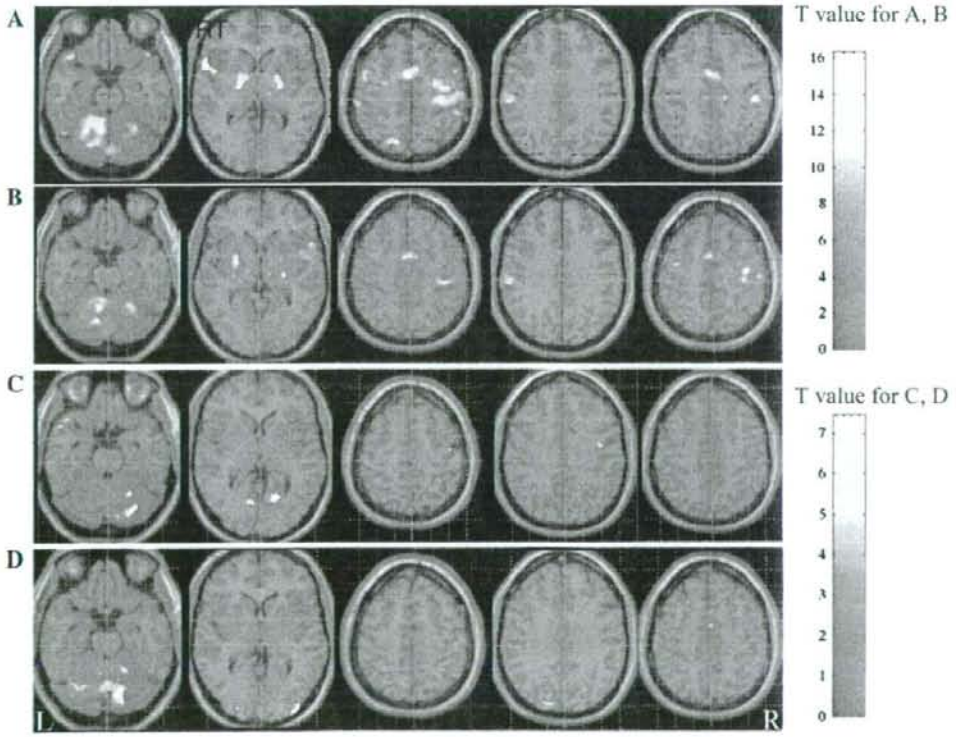

Fig. 2. Regions showing main effects of movement rate (A and B) and significant linear relationship between BOLD signal and increasing movement rate (C and D) in the aged group. All regions are significant at the level of $p < 0.001$, uncorrected. A, C: self-initiated movements; B, D: externally triggered movements in this and subsequent figures.

closed during MRI. Subjects had to (1) make finger-to-thumb opposition movements in the order of index, middle, ring and little fingers; (2) open and clench the fist twice; (3) complete finger-to-thumb opposition movements in the opposite order (namely, little, third, middle and index fingers); (4) once again open and clench the fist twice; and (5) repeat the same series of movements for 40 s during data acquisition. Each individual opposition movement and pair of opening and clenching fist movement was counted as a single movement. During SI tasks, movement rates were set at very slow (as slow as possible), slow, moderate (comfortable pace), fast and very fast (as fast as possible) speeds. During ET tasks, movement rates were set at 0.5, 1, 2, 3 or 4 Hz for all subjects. Subjects paced their movements in response to a metronome, which consisted of a clicking sound at precise time intervals and was delivered binaurally to the subjects via air conduction through a pair of 2.5-m long plastic tubes. During rest conditions, subjects were asked to lie down and listen to the metronome used in the ET session. Movements were performed for 40 s (activation) at a constant rate, followed by 40 s of rest (baseline); the time-point to switch from movement to rest was indicated by a voice signal. Movement rate conditions were presented in a pseudorandom order within an imaging series. Consequently, there were a total of five baseline/activation cycles (for the five different rates) per imaging series. Two consecutive imaging series (one SI, and one ET) were conducted per subject. The order of SI and ET movements was counter-balanced among the subjects. Finger movements were recorded by digital video recording, and exact movement rates were analyzed visually through a video monitor. Two-way analysis of variance (ANOVA) with repeated measures was performed to determine effects of movement rates and tasks.

fMRI methods

Images were acquired on a 1.5 T Magnetom SYMPHONY (Siemens, Enlangen, Germany) whole body MRI system equipped with a circular polarized volume head coil, as previously described (Taniwaki et al., 2003; 2006). Initially, a set of localized images was acquired to position the image slice. In each session, 100 EPI multislice data sets were acquired (TE, 50 ms; TR, 4 s, flip angle, 90°; acquisition time for the whole paradigm, 400 s). Each multislice data set contained 32 transverse slices (slice thickness, 3.0 mm; interslice gap, 1.0 mm; matrix, 64 × 64; FOV, 23 cm). All images were analyzed using SPM 2 Software (Wellcome Department of Cognitive Neurology, London, UK). The first three data sets of each time-series were discarded in order to allow the MRI signal to reach equilibrium, and the remaining EPI volumes were realigned against the first volume. Images were spatially normalized against a standard template and smoothed using a Gaussian kernel with 8-mm full width at half maximum (FWHM). The design matrix was set using the box car reference waveform (40-s epoch). The time-series in each voxel was high-pass filtered (160-s cut-off) and scaled to a grand mean of 100 over voxels and scans within each session.

Activation areas

Activation areas were determined as previously described (Taniwaki et al., 2006). In brief, statistical analysis was performed in two stages. In the first stage, using a single subject fixed effect model and parametric approach in SPM 2, three different rate–response relationships could be identified: (1) categorical on–off responses based on the differences between finger movement and resting conditions regardless of movement rates (zero order term), (2) linear responses in parallel with movement rate (first-order term), and (3) non-linear relationship (second, third and fourth order term) (Büchel et al., 1996, 1998). Each term was represented by the interaction between a delta function and the average of movement rates exerted during each epoch. The resulting covariates were convolved with a canonical synthetic hemodynamic response function and were used in a general linear model (Friston et al., 1995), together with a single covariate representing the mean (constant) term over scans. Parameter estimates for each covariate resulting from the least mean squares fit of the model to the data were calculated, and statistical parametric maps of the *t*-statistic (SPM{*t*}), resulting from linear contrasts of each covariate (Friston et al., 1995), were generated and stored as separate images for each subject.

Table 2
Brain areas with more activation in aged subjects than in young subjects

	Main effect				Linear effect			
	Coordinates				Coordinates			
	Z	*x*	*y*	*z*	*Z*	*x*	*y*	*z*
SI movement								
rPut	n.s.				n.s.			
rGPi	n.s.				n.s.			
rVL	n.s.				n.s.			
rVPL	n.s.				n.s.			
rSMA	n.s.				n.s.			
rSMC	n.s.				n.s.			
rPMv	n.s.				n.s.			
lCB	n.s.				n.s.			
lDN	n.s.				n.s.			
lPut	n.s.				n.s.			
lGPi	n.s.				n.s.			
lVL	n.s.				n.s.			
lVPL	n.s.				n.s.			
lSMA	n.s.				n.s.			
lSMC	3.89	−52	−16	54	n.s.			
lPMv	n.s.				n.s.			
rCB	n.s.				n.s.			
rDN	n.s.				n.s.			
ET movement								
rPut	n.s.				n.s.			
rGPi	n.s.				n.s.			
rVL	n.s.				n.s.			
rVPL	n.s.				n.s.			
rSMA	n.s.				n.s.			
rSMC	n.s.				n.s.			
rPMv	n.s.				n.s.			
lCB	n.s.				n.s.			
lDN	n.s.				n.s.			
lPut	n.s.				n.s.			
lGPi	n.s.				n.s.			
lVL	n.s.				n.s.			
lVPL	n.s.				n.s.			
lSMA	4.08	−10	−18	40	n.s.			
lSMC	4.83	−32	−24	56	n.s.			
lPMv	n.s.				n.s.			
rCB	n.s.				n.s.			
rDN	n.s.				n.s.			

Z-values refer to activation maxima within the respective region, $p < 0.001$ uncorrected, height threshold $Z > 3.09$.

In order to create activation maps representing the main effects of movement rates (0th order), as well as the linear (1st order) and non-linear (2nd, 3rd and 4th order) changes in signals in relation to movement rates, random-effect analysis was performed (Friston et al., 1999). Data for the second stage of analysis comprised pooled parameter estimates for each covariate across all subjects. Contrast images for each subject were entered into a one-sample *t*-test for each covariate of interest. The SPM{*t*} values were thresholded at $p<0.001$ for mapping. For the comparison of activation between the young and aged group, a two-sample *t*-test model ($p<0.001$) was used. Anatomical labels for coordinates in SPM2 (MNI brain template) were defined by Talairach Daemon (http://ric.uthscsa.edu/projects/talairachdaemon.html) after a non-linear transformation of the MNI brain template to the Talairach atlas (http://www.mrc-cbu.cam.ac.uk/Imaging/Common/mnispace.shtml). For SEM, ROIs were selected at the local maxima from the first-order linear effect regardless of the tasks (Taniwaki et al., 2006). Therefore, we investigated the following regions with the following coordinates in young subjects: right putamen (Put) (28, −6, 0), right internal segment of the globus pallidus (GPi) (10, −2, −2), right ventrolateral nucleus of the thalamus (VL) (16, −14, 16), right ventro–posterior–lateral nucleus of the thalamus (VPL) (18, −22, 6), right supplementary motor area (SMA) (6, −2, 40), right sensorimotor cortex (SMC) (48, −20, 52), right ventral premotor cortex (PMv) (52, 2, 38), right dentate nucleus of the cerebellum (DN) (18, −54, −22), right anterior lobe of cerebellar hemisphere (CB) (26, −56, −26), and left Put (−26, −14, 4), left GPi (−12, 0, 0), left VL (−12, −12, 12), left VPL (−12, −20, 8), left SMA (−6, 0, 42), left SMC (−40, −18, 58), left PMv (−56, 0, 32), left DN (−22, −50, −22) and left CB (−30, −54, −22). In aged subjects, some coordinates were also selected at the local maxima from the subjects' first-order linear effect regardless of the tasks: right SMA (2, −4, 48), right SMC (42, −12, 54), right PMv (40, −8, 40), right DN (16, −52, −20), right CB (36, −66, −18), and left VPL (−22, −18, 12), left SMC (−50, −12, 44), left PMv (−56, −8, 38), left DN (−8, −54, −22) and left CB (−26, −68, −16). Other ROIs were selected from the same coordinates in young subjects.

Structural equation modeling

In this analysis, variables were considered in terms of the covariance structure with parameters (interregional connection) being estimated by minimizing the differences between observed covariance and those implied by a predicted model. The model consisted of anatomically separable regions, and connections were specified between those regions and their directions. Anatomical

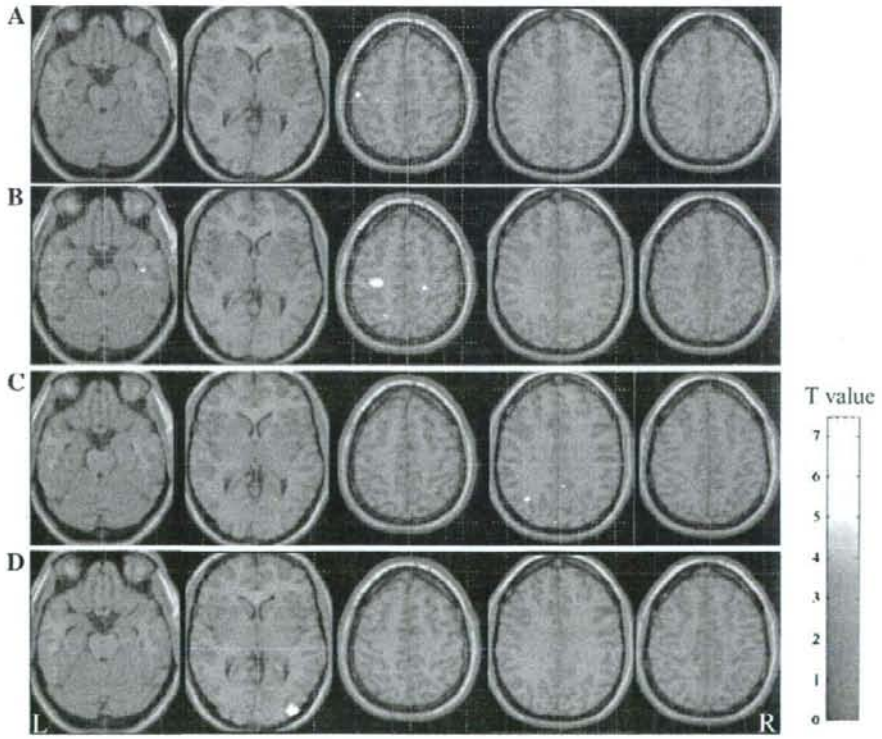

Fig. 3. Brain areas with more activation in aged subjects than in young subjects. Regions showing main effects of movement rate (A and B) and a significant linear relationship between BOLD signal and increasing movement rate (C and D). All regions are significant at the level of $p<0.001$, uncorrected.

regions comprised Put, GPi, VL, VPL, SMA, SMC, PMv, CB and DN (Table 1). Connections between brain regions are based on the neuroanatomical knowledge of BGTM and CC loops (Alexander et al., 1990; Delong, 1990; Kelly and Strick, 2003) as described previously (Taniwaki et al., 2006). The basal ganglia–thalamo–motor (BGTM) loop comprises some cortical motor areas, including the SMA, PMv and SMC, and several subcortical structures such as the Put, GPi and VL. The Put is the input nucleus of the basal ganglia and receives projections from SMA, PMv and SMC. The GPi receives input from the Put and is considered to be an output nucleus of the basal ganglia. In turn, the VL receives projections from the GPi and completes the circuit by projecting back to the SMA, PMv and SMC (Alexander et al., 1990; Delong, 1990). In the cerebello-cerebral (CC) loop, motor cortices such as SMC or PMv are target structures of outputs from the CB via the DN and VPL, while cerebellar inputs originate from these motor cortices (Kelly and Strick, 2003). Between the two loops, SMA and PMv have reciprocal interconnections with each other and project to SMC (Barbas and Pandya, 1987; Johnson et al., 1996; Muakkassa and Strick, 1979; Rizzolatti et al., 1998; Rowe et al., 2002). Recursive connections from the cortex back to the thalamus have also been documented in such a model (Delong, 1990; Grafton et al., 1994). Since significant linear effects were observed in bilateral hemispheres, it was decided to construct an anatomical network for bilateral loops. Interhemispheric connections were constructed by a primate study within motor cortices, such as the SMC, PMv and SMA (Rouiller et al., 1994). A schematic representation of all of the connections used in this study is shown in Fig. 1.

fMRI signal changes were calculated using a single subject fixed effect model. Averaged signal changes of baseline epochs were subtracted from those of each task condition. fMRI data of local maxima in each ROI were standardized to zero mean and to unit variance for each participant (Bullmore et al., 2000; Kondo et al., 2004). The individual time-series for each location were then concatenated into a group matrix for path analysis and subsequent group comparisons ($n=1164$) to obtain stable SEM model solutions. Interregional correlations of activity between selected regions were obtained and the pairwise correlations $c_{i,j}$ for the ith and jth regions constituted the $(p \times p)$ interregional correlation matrix. The matrix was combined with a neuroanatomical model (Fig. 1) to compute structural equation models using LISREL 8.5 software (Scientific Software International, Inc, Lincolnwood, IL). A maximum likelihood algorithm was used to fit the parameters. Within-hemisphere functional networks were constructed at first, and the functional network accounting for interhemispheric interactions was calculated in the final stage (McIntosh et al., 1994). The influence of other connections could be estimated by modification indices (McIntosh and Gonzalez-Lima, 1994; McIntosh et al., 1994). Residual influences were set to 0.30 for all regions. Statistical inferences from group differences were based on a stacked model approach including an omnibus test. This procedure determined the χ^2 goodness-of-fit statistic for both a null model, in which path coefficients are equally constrained between conditions, and an alternative model, in which coefficients are allowed to differ (McIntosh et al., 1994). The significance of differences between the models was expressed as the difference in the χ^2 statistic with degrees of freedom equal to differences in the degrees of freedom for the null model and alternative models (McIntosh et al., 1994).

Results

Performance of subjects

During SI movements in aged subjects, very slow movements were performed at a frequency of 1.00±0.37 Hz (mean±SD), slow movements were performed at a rate of 1.26±0.46 Hz, moderate movements were performed at 1.75±0.59 Hz, fast movements were performed at 2.87±0.53 Hz, and very fast movements were performed at 3.43±0.63 Hz. ET movement rates were almost identical to the rates of the auditory triggers (0.5 Hz trigger, 0.56±0.14 Hz; 1 Hz trigger, 0.98±0.04 Hz; 2 Hz trigger, 1.98±0.04 Hz; 3 Hz trigger, 2.94±0.09 Hz; 4 Hz trigger, 3.78±0.16 Hz). In our previous reports of young subjects (Taniwaki et al., 2006), very slow movements were performed at a frequency of

Table 3
Brain areas with more activation in young subjects than in aged subjects

	Main effect				Linear effect			
	Coordinates				Coordinates			
	Z	*x*	*y*	*z*	*Z*	*x*	*y*	*z*
SI movement								
rPut	n.s.				4.19	26	−8	−2
rGPi	n.s.				n.s.			
rVL	n.s.				3.18	8	−14	2
rVPL	n.s.				4.02	16	−22	6
rSMA	n.s.				3.22	4	−2	42
rSMC	3.55	56	−18	46	n.s.			
rPMv	n.s.				n.s.			
lCB	n.s.				n.s.			
lDN	n.s.				n.s.			
lPut	n.s.				n.s.			
lGPi	n.s.				n.s.			
lVL	n.s.				n.s.			
lVPL	n.s.				n.s.			
lSMA	n.s.				3.19	−4	4	44
lSMC	n.s.				n.s.			
lPMv	n.s.				n.s.			
rCB	n.s.				n.s.			
rDN	n.s.				n.s.			
ET movement								
rPut	n.s.				n.s.			
rGPi	n.s.				n.s.			
rVL	n.s.				n.s.			
rVPL	n.s.				n.s.			
rSMA	n.s.				n.s.			
rSMC	n.s.				n.s.			
rPMv	n.s.				n.s.			
lCB	3.84	−26	−50	−20	n.s.			
lDN	n.s.				n.s.			
lPut	n.s.				n.s.			
lGPi	n.s.				n.s.			
lVL	n.s.				n.s.			
lVPL	n.s.				n.s.			
lSMA	n.s.				n.s.			
lSMC	n.s.				n.s.			
lPMv	n.s.				n.s.			
rCB	n.s.				n.s.			
rDN	n.s.				n.s.			

Z-values refer to activation maxima within the respective region, $p<0.001$ uncorrected, height threshold $Z>3.09$.

0.69±0.16 Hz (mean±SD), slow movements were performed at 1.00±0.25 Hz, moderate movements were performed at 1.84±0.58 Hz, fast movements were performed at 2.95±0.78 Hz, and very fast movements were performed at 4.03±0.94 Hz during SI movements; as in the present study, ET movement rates were almost identical to the rates of the auditory triggers (0.5 Hz trigger, 0.51±0.02 Hz; 1 Hz trigger, 1.00±0.01 Hz; 2 Hz trigger, 1.99±0.02 Hz; 3 Hz trigger, 3.01±0.07 Hz; 4 Hz trigger, 3.97±0.07 Hz). No statistical difference was observed between young and aged subjects ($p=0.626$ in SI movements and $p=0.131$ in ET movements, determined by two-way ANOVA with repeated measures), although there was a tendency toward slower movement during the SI task and increased variability in frequency during ET task in aged subjects compared with young subjects.

Foci of activation

Within group analysis in aged subjects

To separate regional activities within the same task but with different rate–response functions, a parametric approach based on orthogonal basic functions up to the fourth order was used. In the study of main effects, both tasks caused significant activation in the bilateral posterior Put, VL, VPL, SMA, SMC, PMv, DN, CB and the right GP (Table 1; Figs. 2A and B) in the aged subjects, consistent with the results in young subjects previously reported (Taniwaki et al., 2006).

A significant positive linear increase in the magnitude of the BOLD response in parallel with rate of finger movement was seen in the right SMC, PMv and DN, and the left VPL, SMC and PMv during SI tasks (Table 1; Fig. 2C). There was a tendency toward a linear increase in the activation of the left CB. In ET tasks, a significant positive linear increase was detected in the right SMA, left SMC, bilateral CB and DN, and a tendency toward a linear increase in activation was observed in the right SMC and PMv (Table 1; Fig. 2D).

Neither a significant non-linear rate–response function (2nd order), nor a negative linear correlation in terms of a decline in BOLD response in parallel with tapping rate, was documented in BGTM or CC loops.

Between-group analysis of brain activity

Compared with young subjects, aged subjects had greater activation in the left SMC during SI tasks and in the left SMA and SMC during ET tasks in a study of main effects (Table 2; Fig. 3). There was greater activation in the right SMC during SI tasks and in the left CB during ET tasks in young subjects compared with aged subjects in the main effects analysis (Table 3; Fig. 4). In the analysis of linear effects, young subjects showed greater

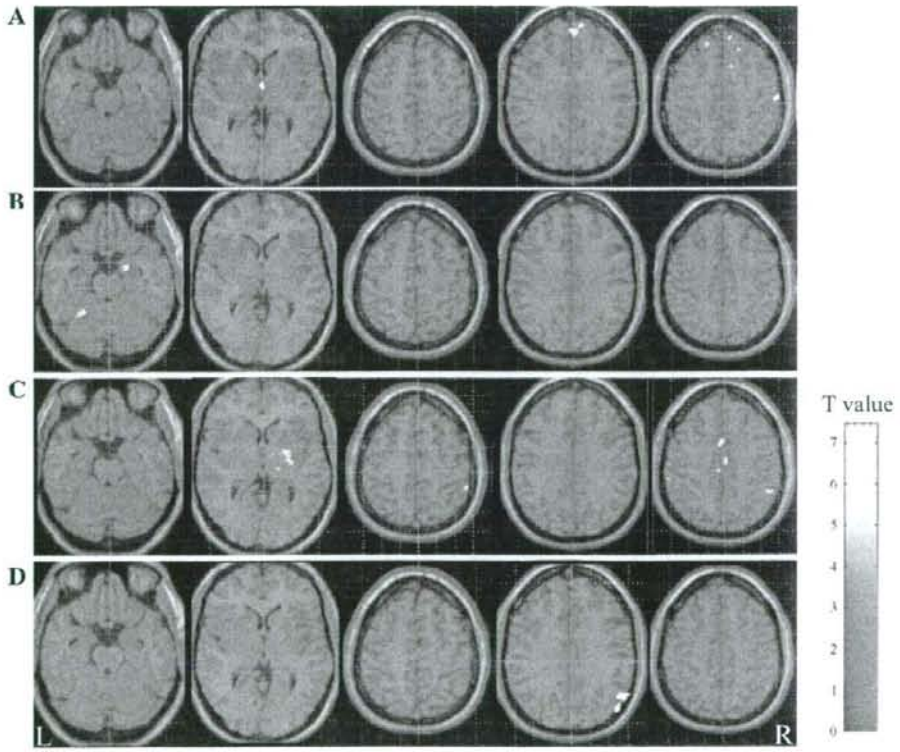

Fig. 4. Brain areas with more activation in young subjects than in aged subjects. Regions showing main effects of movement rate (A and B) and a significant linear relationship between BOLD signal and increasing movement rate (C and D). All regions are significant at the level of $p<0.001$, uncorrected.

activation in the right Put, VL, VPL, SMA and left SMA during SI movement.

Structural equation modeling

The results of mapping experiments on aged subjects suggest that the bilateral motor cortices contribute more to the rate-dependent motor processing than the subcortical motor loops. To confirm this hypothesis, functional network analysis was performed.

Within-group analysis of structural equation modeling in aged subjects

The omnibus test showed that the functional networks in the right hemisphere and left cerebellum differed significantly between the two tasks in aged subjects [χ^2 diff(29)=387.37, $p<0.001$]. Functional interactions from the right SMC to the right VL, and those from the right PMv to the right SMC were stronger during SI tasks. There were moderate interactions from the right SMA to the right SMC during both tasks (Table 5; Figs. 5C and D).

Functional networks in the left hemisphere and right cerebellum differed significantly between the two tasks according to the omnibus test [χ^2 diff(29)=327.54, $p<0.001$]. Interactions from the left GPi to the left VL were stronger during SI tasks, whereas those from the left PMv to the left SMA were stronger during ET tasks.

Interhemisphere SEM in SI tasks resulted in a model that was different from that generated during the ET task [χ^2 diff(12)=271.01, $p<0.001$]. Interactions from the left to right PMv were stronger during SI movements; by contrast, the interactions from the right SMA to the left SMC, those from the left to right SMC, and those from the left SMA to right PMv were stronger during ET tasks. Moderate interactions between both SMAs were observed in both tasks.

Between-group analysis of structural equation modeling

The functional networks in the right hemisphere and left cerebellum differed significantly between the two groups of subjects according to the omnibus test of data collected during SI tasks [χ^2 diff(29)=1078.72, $p<0.001$] and ET tasks [χ^2 diff(29)=280.71, $p<0.001$]. During SI tasks, BGTM interactions from the right SMA to the right SMC, via the right Put, right GPi and right VL, were stronger in young subjects than in aged subjects, whereas the interactions from the right SMA to the right SMC

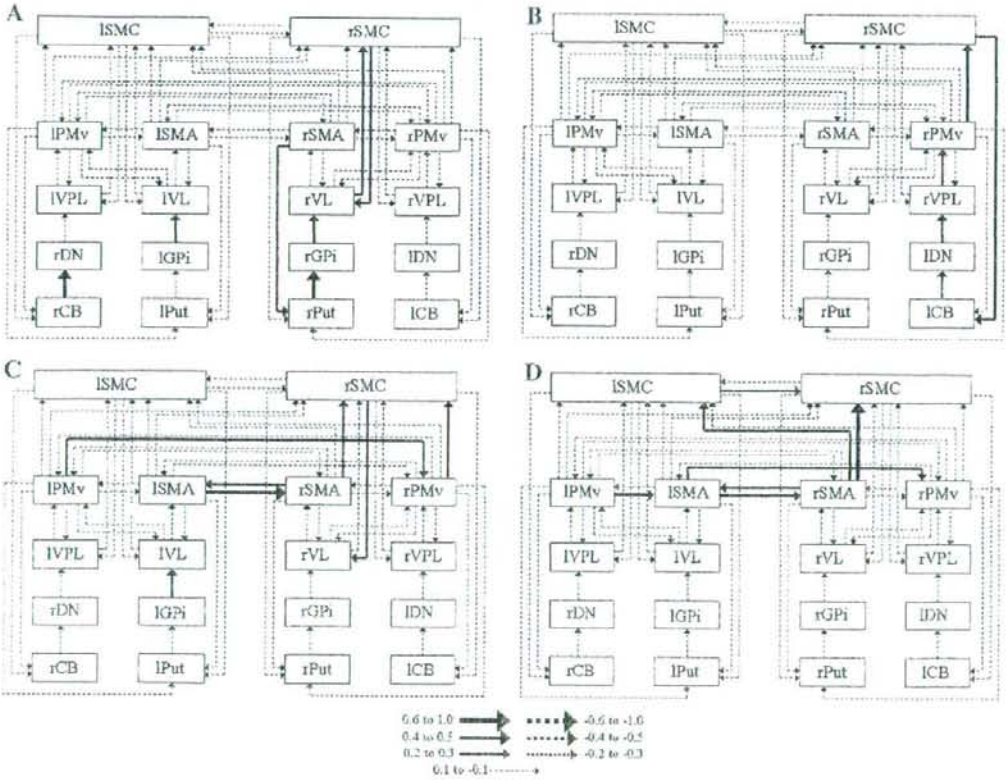

Fig. 5. Schematic representation of the results of structural equation modeling in young (A and B) and aged subjects (C and D). (A and C) Self-initiated movements. (B and D) Externally triggered movements. Positive coefficients (solid arrows) indicate interactions in which an increase in activity in one area is associated with an increase in activity in the other area. Negative coefficients (broken arrows) indicate opposite interactions.

Table 4
Interregional correlation coefficients (Pearson product-moment correlation (A) and path coefficients (B) during two different tasks in young subjects

	rPut	rGP	rVL	rVPL	rSMA	rSMC	rPMv	lDN	lCB	lPut	lGP	lVL	lVPL	lSMA	lSMC	lPMv	rDN	rCB
A																		
	SI																	
rPut	1.00																	
rGP	0.53	1.00																
rVL	0.05	0.26	1.00															
rVPL	0.19	0.20	0.17	1.00														
rSMA	0.24	0.06	0.11	0.00	1.00													
rSMC	0.00	0.04	0.33	0.06	−0.03	1.00												
rPMv	0.10	−0.02	0.17	0.03	−0.01	0.21	1.00											
lDN	0.25	0.16	0.00	0.17	0.04	0.00	−0.03	1.00										
lCB	0.21	0.08	0.08	0.10	0.06	0.17	0.01	0.18	1.00									
lPut	0.20	0.25	−0.01	0.22	−0.02	−0.12	0.07	0.16	0.02	1.00								
lGP	0.14	0.16	0.14	0.17	−0.07	0.13	0.11	0.21	0.06	0.17	1.00							
lVL	0.11	0.13	0.46	0.18	0.16	0.17	0.09	0.05	0.07	0.06	0.21	1.00						
lVPL	0.11	0.16	0.28	0.33	0.09	0.01	0.03	0.15	0.02	0.16	0.16	0.42	1.00					
lSMA	0.12	0.11	0.03	−0.01	0.18	−0.06	0.03	0.07	−0.05	0.08	0.00	0.14	0.04	1.00				
lSMC	0.05	0.06	0.05	0.03	0.17	0.20	0.01	0.12	0.07	−0.03	0.04	0.16	0.06	0.02	1.00			
lPMv	0.07	0.07	−0.02	0.12	0.15	0.03	−0.02	0.14	−0.02	0.07	0.09	−0.03	0.03	0.14	0.16	1.00		
rDN	0.26	0.21	0.06	0.16	0.08	0.02	−0.02	0.43	0.21	0.10	0.21	0.16	0.06	0.03	0.07	0.02	1.00	
rCB	0.08	0.00	−0.09	−0.08	0.06	0.01	−0.03	0.05	0.29	0.06	−0.02	0.02	−0.04	0.06	0.09	0.00	0.41	1.00
	ET																	
rPut	1.00																	
rGP	0.17	1.00																
rVL	−0.01	0.16	1.00															
rVPL	0.01	0.18	0.35	1.00														
rSMA	−0.02	0.14	0.17	0.08	1.00													
rSMC	0.11	0.10	0.12	0.10	0.13	1.00												
rPMv	0.17	0.06	0.04	0.23	0.04	0.22	1.00											
lDN	0.23	0.15	0.12	0.22	0.06	0.12	0.00	1.00										
lCB	0.02	−0.06	0.16	0.04	0.09	0.28	0.08	0.26	1.00									
lPut	0.16	0.09	0.07	0.11	0.11	0.11	0.11	0.14	0.00	1.00								
lGP	0.10	0.19	0.20	0.18	0.14	0.06	0.04	0.11	0.05	0.13	1.00							
lVL	−0.10	0.23	0.25	0.21	0.15	0.03	0.16	0.03	0.00	0.08	0.15	1.00						
lVPL	0.19	0.33	0.28	0.26	0.07	−0.01	0.17	0.19	0.02	0.14	0.26	0.50	1.00					
lSMA	0.10	0.14	0.12	0.03	0.17	0.10	0.09	0.03	−0.03	0.02	0.12	0.14	0.15	1.00				
lSMC	0.29	0.06	−0.12	−0.05	0.08	0.15	0.17	0.16	0.14	−0.04	−0.03	0.02	0.10	0.10	1.00			
lPMv	0.08	0.02	0.01	−0.06	0.06	0.06	0.11	−0.06	0.08	0.08	0.03	0.01	0.04	0.11	0.05	1.00		
rDN	0.16	−0.12	−0.13	0.00	0.00	0.08	−0.03	0.33	0.18	0.11	0.10	0.07	0.12	0.02	0.15	0.05	1.00	
rCB	0.05	−0.09	−0.04	0.00	−0.06	−0.04	0.00	0.10	0.22	−0.09	−0.02	0.03	−0.04	−0.06	0.08	−0.02	0.18	1.00
B																		
	SI																	
rPut	–	–	–	–	0.24	−0.03	0.10	–	–	–	–	–	–	–	–	–	–	–
rGP	0.53	–	–	–	–	–	–	–	–	–	–	–	–	–	–	–	–	–
rVL	–	0.24	–	–	0.08	0.22	0.09	–	–	–	–	–	–	–	–	–	–	–
rVPL	–	–	–	–	–	0.06	0.03	0.17	–	–	–	–	–	–	–	–	–	–
rSMA	–	–	0.08	–	–	–	−0.02	–	–	–	–	–	–	0.12	–	0.10	–	–
rSMC	–	–	0.24	0.01	0.06	–	0.16	–	–	–	–	–	–	−0.07	0.15	0.02	–	–
rPMv	–	–	0.13	0.00	−0.02	–	–	–	–	–	–	–	–	0.03	–	−0.02	–	–
lDN	–	–	–	–	–	–	–	–	0.18	–	–	–	–	–	–	–	–	–
lCB	–	–	–	–	–	0.18	−0.03	–	–	–	–	–	–	–	–	–	–	–
lPut	–	–	–	–	–	–	–	–	–	–	–	–	–	0.07	−0.04	0.07	–	–
lGP	–	–	–	–	–	–	–	–	–	0.17	–	–	–	–	–	–	–	–
lVL	–	–	–	–	–	–	–	–	–	–	0.21	–	–	0.12	0.12	−0.07	–	–
lVPL	–	–	–	–	–	–	–	–	–	–	–	–	–	–	0.09	−0.05	0.06	–
lSMA	–	–	–	–	0.14	–	0.02	–	–	–	–	0.11	–	–	–	0.11	–	–
lSMC	–	–	–	–	0.17	0.16	−0.02	–	–	–	–	0.15	−0.03	−0.03	–	0.17	–	–
lPMv	–	–	–	–	0.12	–	−0.01	–	–	–	–	−0.06	0.06	0.11	–	–	–	–
rDN	–	–	–	–	–	–	–	–	–	–	–	–	–	–	–	–	–	0.41
rCB	–	–	–	–	–	–	–	–	–	–	–	–	–		0.09	−0.02	–	–

(continued on next page)

Table 4 (*continued*)

	rPut	rGP	rVL	rVPL	rSMA	rSMC	rPMv	lDN	lCB	lPut	lGP	lVL	lVPL	lSMA	lSMC	lPMv	rDN	rCB
B																		
	ET																	
rPut	–	–	–	–	−0.04	0.08	0.15	–	–	–	–	–	–	–	–	–	–	–
rGP	0.17	–	–	–	–	–	–	–	–	–	–	–	–	–	–	–	–	–
rVL	–	0.14	–	–	0.10	0.06	0.03	–	–	–	–	–	–	–	–	–	–	–
rVPL	–	–	–	–	–	0.02	−0.02	0.21	–	–	–	–	–	–	–	–	–	–
rSMA	–	–	0.14	–	–	–	0.03	–	–	–	–	–	–	0.13	–	0.03	–	–
rSMC	–	–	0.07	0.01	0.11	–	0.21	–	–	–	–	–	–	0.08	0.12	0.05	–	–
rPMv	–	–	−0.07	0.26	0.02	–	–	–	–	–	–	–	–	0.06	–	0.08	–	–
lDN	–	–	–	–	–	–	–	–	0.26	–	–	–	–	–	–	–	–	–
lCB	–	–	–	–	–	0.28	0.02	–	–	–	–	–	–	–	–	–	–	–
lPut	–	–	–	–	–	–	–	–	–	–	–	–	–	0.02	−0.05	0.08	–	–
lGP	–	–	–	–	–	–	–	–	–	0.13	–	–	–	–	–	–	–	–
lVL	–	–	–	–	–	–	–	–	–	–	0.14	–	–	0.09	0.03	0.00	–	–
lVPL	–	–	–	–	–	–	–	–	–	–	–	–	–	–	−0.06	−0.01	0.13	–
lSMA	–	–	–	–	0.13	–	0.07	–	–	–	–	0.11	–	–	–	0.08	–	–
lSMC	–	–	–	–	−0.07	0.07	0.15	–	–	–	–	−0.07	0.14	0.08	–	0.04	–	–
lPMv	–	–	–	–	−0.05	–	0.08	–	–	–	–	−0.03	0.04	0.08	–	–	–	–
rDN	–	–	–	–	–	–	–	–	–	–	–	–	–	–	–	–	–	0.18
rCB	–	–	–	–	–	–	–	–	–	–	–	–	–	–	0.08	−0.02	–	–

and those from the right PMv to right SMC were stronger in aged subjects. There were moderate interactions from the right SMC to the right VL in both subjects. During ET tasks, entire CC interactions from the left CB to the left CB, via the left DN, right VPL, right PMv and right SMC, were stronger in young subjects. By contrast, interaction from the right SMA to the right SMC was stronger in aged subjects (Tables 4, 5; Fig. 5).

The omnibus test suggested that the functional networks of the left hemisphere and right cerebellum are different between the young and aged groups during both SI [χ^2 diff(29)=344.92, $p<0.001$] and ET tasks [χ^2 diff(29)=255.01, $p<0.001$]. During SI tasks, moderate interactions were seen from the left GPi to the left VL in both groups. In addition, the interactions from the right CB to the right DN were stronger in the young group than in the aged group. During ET tasks, the interactions from the left PMv to the left SMA were stronger in the aged group.

The results of interhemisphere SEM were different between young and aged groups during both SI [χ^2 diff(12)=2013.49, $p<0.001$] and ET tasks [χ^2 diff(12)=2404.69, $p<0.001$]. Only the old group showed moderate interactions between hemispheres. During SI tasks, there were stronger interactions from the left PMv to right PMv in the aged group. During ET tasks, interhemispheric interactions from the left SMA to right PMv, those from the left SMC to the right SMC and those from the right SMA to the left SMC were stronger in the aged group. There were stronger reciprocal influences among bilateral SMAs in the aged group during both tasks.

Discussion

In the current study, we compared functional interactions within the BGTM and CC loops between young and aged subjects using fMRI combined with a parametric approach and SEM, during sequential finger movements of SI and ET tasks. The major new findings in aged subjects were as follows: (1) decreased connectivity within BGTM loops during SI movements, (2) decreased connectivity within CC loops during ET movements and (3) increased connectivity within motor cortices and between hemispheres during both types of movement.

Decreased connectivity within BGTM loop during SI task

Normal aging is characterized by impaired motor ability (Calautti et al., 2001; Mattay et al., 2002; Sailer et al., 2000; Welford, 1988). In particular, slowing of motor movements and loss of fine motor skills are thought to reflect underlying age-related degeneration in brain systems subserving motor function (Smith et al., 1999). The basal ganglia are subcortical nuclei that are thought to be motor structures involved in the timing of movements (O'Boyle et al., 1996; Pastor et al., 1992, 2004), the speed of movement and the acquisition of motor skills (Laforce and Doyon, 2002; Vakil et al., 2000). Concerning the contribution of lower sensorimotor processes to behavioral slowing in the elderly, Kaasinen et al. (2000) have documented the decline of the dopaminergic neurotransmitter system in the aging human brain and, more specifically, the loss of dopamine receptors in the striatum and extrastriatal regions, which is associated with a basic impairment in motor functions (Volkow et al., 1998). These results suggest decreased activity in the regions within the BGTM loop in aged subjects.

Although several functional brain imaging studies have reported age-related changes in human motor system, only a few studies have reported age-related changes in the striatum. In an fMRI study of a visually paced button press task using the right hand, aged subjects showed additional areas of activation in the bilateral Put (Mattay et al., 2002). Aged subjects showed greater *activation* in the ipsilateral Put and less activation in the contralateral Put, when either making a fist or opposing the thumb and index finger with left hand (Fang et al., 2005). Studies of self-initiated, memorized sequential right finger movements (Wu and Hallett, 2005), visually paced isometric hand grip tasks using each hand (Ward and Frackowiak, 2003), auditory paced finger and wrist movements of each hand (Hutchinson et al., 2002) and auditory paced thumb to index tapping with either hand (Calautti et al., 2001) failed to show any age-related change in the activation of the striatum. Thus, the results of previous functional brain imaging studies were inconsistent. Basically, these studies performed categorical comparisons of fMRI and PET data and could only show the change in activation in each

Table 5
Interregional correlation coefficients (Pearson product-moment correlation (A) and path coefficients (B) during two different tasks in aged subjects

	rPut	rGP	rVL	rVPL	rSMA	rSMC	rPMv	lDN	lCB	lPut	lGP	lVL	lVPL	lSMA	lSMC	lPMv	rDN	rCB
A																		
	SI																	
rPut	1.00																	
rGP	0.19	1.00																
rVL	0.18	0.16	1.00															
rVPL	0.27	0.20	0.29	1.00														
rSMA	0.05	0.02	0.02	0.02	1.00													
rSMC	0.17	0.08	0.26	0.21	0.30	1.00												
rPMv	0.10	0.13	0.19	0.11	0.12	0.29	1.00											
lDN	0.08	0.05	0.19	0.18	0.10	0.21	0.14	1.00										
lCB	0.00	0.03	0.15	0.04	−0.02	0.05	−0.04	0.15	1.00									
lPut	0.25	0.22	0.13	0.18	−0.05	0.03	0.18	0.13	0.10	1.00								
lGP	0.21	0.30	0.27	0.19	0.09	0.06	0.15	0.05	0.10	0.17	1.00							
lVL	0.13	0.24	0.54	0.27	0.00	0.10	0.11	0.15	0.16	0.18	0.30	1.00						
lVPL	0.25	0.22	0.38	0.28	0.01	0.12	0.15	0.15	0.19	0.26	0.27	0.52	1.00					
lSMA	0.09	0.09	−0.01	0.04	0.55	0.21	0.14	0.07	−0.07	0.02	0.06	−0.02	0.01	1.00				
lSMC	0.06	0.06	0.04	0.07	0.03	0.09	0.19	0.09	−0.02	0.12	0.06	0.04	0.13	0.12	1.00			
lPMv	0.16	0.21	0.18	0.16	0.09	0.19	0.28	0.14	0.00	0.08	0.11	0.15	0.08	0.20	0.17	1.00		
rDN	0.08	0.05	0.15	0.11	0.09	0.20	0.20	0.37	0.21	0.05	0.04	0.13	0.10	0.04	0.05	0.10	1.00	
rCB	−0.01	0.04	0.05	0.01	−0.05	−0.01	−0.04	0.11	0.49	0.12	−0.01	0.12	0.22	−0.04	0.02	−0.04	0.13	1.00
	ET																	
rPut	1.00																	
rGP	0.06	1.00																
rVL	0.13	0.00	1.00															
rVPL	0.15	0.16	0.20	1.00														
rSMA	0.08	0.00	0.06	0.08	1.00													
rSMC	0.03	0.00	0.04	0.08	0.46	1.00												
rPMv	0.05	0.09	0.03	0.10	0.24	0.20	1.00											
lDN	0.12	0.08	0.17	0.13	0.07	0.15	0.09	1.00										
lCB	0.04	0.03	0.10	0.01	0.12	−0.02	−0.05	0.10	1.00									
lPut	0.09	0.20	0.13	0.26	0.06	0.02	0.03	0.11	0.09	1.00								
lGP	0.16	0.21	0.09	0.17	0.01	0.05	0.01	0.08	0.07	0.10	1.00							
lVL	0.12	0.11	0.53	0.19	0.13	0.09	0.07	0.17	0.09	0.16	0.05	1.00						
lVPL	0.15	0.02	0.28	0.21	0.04	0.01	0.05	0.14	0.01	0.20	0.08	0.33	1.00					
lSMA	0.16	0.01	0.07	0.00	0.49	0.20	0.28	0.08	0.04	0.03	−0.02	0.08	0.13	1.00				
lSMC	0.07	−0.05	0.18	0.09	0.36	0.34	0.07	0.10	0.18	0.10	0.08	0.11	0.09	0.18	1.00			
lPMv	0.11	0.08	0.11	0.09	0.15	0.03	0.15	0.05	−0.03	0.08	0.03	0.08	0.17	0.26	0.11	1.00		
rDN	0.12	0.04	0.10	0.20	−0.07	0.00	0.03	0.28	0.12	0.11	−0.07	0.14	0.12	−0.01	0.03	−0.01	1.00	
rCB	0.02	0.03	0.10	−0.01	−0.12	−0.13	0.00	0.03	0.33	0.05	0.01	0.05	−0.04	0.01	−0.02	0.04	0.06	1.00
B																		
	SI																	
rPut	–	–	–	–	0.00	0.15	0.05	–	–	–	–	–	–	–	–	–	–	–
rGP	0.19	–	–	–	–	–	–	–	–	–	–	–	–	–	–	–	–	–
rVL	–	0.13	–	–	−0.06	0.20	0.08	–	–	–	–	–	–	–	–	–	–	–
rVPL	–	–	–	–	–	0.01	0.01	0.18	–	–	–	–	–	–	–	–	–	–
rSMA	–	–	0.00	–	–	–	0.09	–	–	–	–	–	–	0.41	–	−0.02	–	–
rSMC	–	–	0.11	0.15	0.27	–	0.21	–	–	–	–	–	–	0.18	0.04	0.15	–	–
rPMv	–	–	0.13	0.07	0.09	–	–	–	–	–	–	–	–	0.08	–	0.20	–	–
lDN	–	–	–	–	–	–	–	–	0.15	–	–	–	–	–	–	–	–	–
lCB	–	–	–	–	–	0.07	−0.06	–	–	–	–	–	–	–	–	–	–	–
lPut	–	–	–	–	–	–	–	–	–	–	–	–	–	−0.01	0.11	0.06	–	–
lGP	–	–	–	–	–	–	–	–	–	0.17	–	–	–	–	–	–	–	–
lVL	–	–	–	–	–	–	–	–	–	–	0.29	–	–	−0.05	0.04	0.08	–	–
lVPL	–	–	–	–	–	–	–	–	–	–	–	–	–	–	−0.07	0.10	0.09	–
lSMA	–	–	–	–	0.39	–	0.06	–	–	–	–	−0.03	–	–	–	0.16	–	–
lSMC	–	–	–	–	0.00	0.03	0.18	–	–	–	–	−0.09	0.18	0.09	–	0.15	–	–
lPMv	–	–	–	–	0.07	–	0.21	–	–	–	–	0.14	−0.02	0.15	–	–	–	–
rDN	–	–	–	–	–	–	–	–	–	–	–	–	–	–	–	–	–	0.13
rCB	–	–	–	–	–	–	–	–	–	–	–	–	–	–	0.03	−0.04	–	–

(continued on next page)

Table 5 (*continued*)

	rPut	rGP	rVL	rVPL	rSMA	rSMC	rPMv	lDN	lCB	lPut	lGP	lVL	lVPL	lSMA	lSMC	lPMv	rDN	rCB
B																		
	ET																	
rPut	–	–	–	–	0.08	−0.01	0.03	–	–	–	–	–	–	–	–	–	–	–
rGP	0.06	–	–	–	–	–	–	–	–	–	–	–	–	–	–	–	–	–
rVL	–	0.00	–	–	0.04	0.01	0.02	–	–	–	–	–	–	–	–	–	–	–
rVPL	–	–	–	–	–	0.02	0.00	0.13	–	–	–	–	–	–	–	–	–	–
rSMA	–	–	0.04	–	–	–	0.18	–	–	–	–	–	–	0.37	–	0.01	–	–
rSMC	–	–	0.00	0.03	0.44	–	0.09	–	–	–	–	–	–	0.16	0.28	−0.04	–	–
rPMv	–	–	−0.01	0.09	0.18	–	–	–	–	–	–	–	–	0.22	–	0.06	–	–
lDN	–	–	–	–	–	–	–	–	0.10	–	–	–	–	–	–	–	–	–
lCB	–	–	–	–	–	−0.01	−0.05	–	–	–	–	–	–	–	–	–	–	–
lPut	–	–	–	–	–	–	–	–	–	–	–	–	–	−0.01	0.09	0.07	–	–
lGP	–	–	–	–	–	–	–	–	–	0.10	–	–	–	–	–	–	–	–
lVL	–	–	–	–	–	–	–	–	–	–	0.04	–	–	0.04	0.07	0.06	–	–
lVPL	–	–	–	–	–	–	–	–	–	–	–	–	–	–	0.05	0.03	0.12	–
lSMA	–	–	–	–	0.33	–	0.12	–	–	–	–	0.04	–	–	–	0.20	–	–
lSMC	–	–	–	–	0.31	0.11	−0.03	–	–	–	–	0.06	0.03	0.16	–	0.06	–	–
lPMv	–	–	–	–	0.12	–	0.10	–	–	–	–	0.00	0.14	0.18	–	–	–	–
rDN	–	–	–	–	–	–	–	–	–	–	–	–	–	–	–	–	–	0.06
rCB	–	–	–	–	–	–	–	–	–	–	–	–	–	–	−0.02	0.04	–	–

region. Instead, we used correlation data based on rate-dependent movements and SEM. SEM has provided new insights into task-specific functional networks (Grafton et al., 1994; McIntosh and Gonzalez-Lima, 1994; McIntosh et al., 1994). Our approach provides additional information about brain physiology such as rhythm formation, motor preparation and motor execution that is not always apparent in the results of categorical comparisons of fMRI data (Taniwaki et al., 2006). Consistent with clinical (Smith et al., 1999) and pathological studies (Kaasinen et al., 2000; Volkow et al., 1998), our current mapping study shows less activation in the right Put, VL and bilateral SMA in the aged group compared with the young group during SI movements. Our SEM results further indicate an age-dependent decline in connectivity within BGTM loops during SI tasks. To our knowledge, we are the first to show an age-related decrease in connectivity within the BGTM loop. Our aged group also showed the tendency toward slower movement during the SI task. Because the BGTM loop is suggested to play an important role in central timing processes (in the SMA, basal ganglia and VL) and execution processes in the SMC (Taniwaki et al., 2003; 2006), age-related decline of either central timing processes and/or execution processes might reflect the decreased connectivity within BGTM loop and slower movement during the SI task.

Decreased connectivity within the CC loop during ET tasks

The cerebellum also plays an important role as a motor structure (Casini and Ivry, 1999; Ivry et al., 1988; Laforce and Doyon, 2002) and is involved in the execution of fine motor skills which are lost during aging (Smith et al., 1999). *Anatomically*, significant changes are observed with age in the anterior lobe, where a selective 40% loss of both Purkinje and granule cells was observed in the cerebellum. Furthermore, a 30% loss of volume, mostly due to loss of cortical volume, was observed in the anterior lobe, which is predominantly involved in motor control (Andersen et al., 2003). Thus, decreased activity within the CC loop can be predicted.

Several functional brain imaging studies have reported age-related changes in the cerebellum. fMRI studies of a visually paced button press task using right hand (Mattay et al., 2002) and self-initiated, memorized sequential right finger movements (Wu and Hallett, 2005) demonstrated greater activation in the bilateral cerebellar cortex in aged subjects compared with young subjects. In an fMRI study of a visually paced isometric hand grip task using each hand, aged subjects showed additional areas of activation in the cerebellar vermis (Ward and Frackowiak, 2003). By contrast, aged subjects showed less activation in bilateral cerebellum by auditory paced right finger or wrist movement and in the left cerebellum during left wrist movement compared with young subjects in an fMRI study (Hutchinson et al., 2002). A PET study also showed no age-related change in the cerebellum during auditory paced thumb to index tapping with either hand (Calautti et al., 2001). Previous imaging studies of regional activation in the cerebellum have failed to show consistent results, though the tasks were different from each other.

Consistent with clinical study (Smith et al., 1999) and anatomical study (Andersen et al., 2003), our SEM results indicate an age-dependent decline in connectivity within CC loops during ET tasks. Our aged group also showed the tendency toward increased variability in frequency in the ET task. Because the CC loop is involved in the functions of the cerebellum in monitoring and adjusting inputs from SMC, as well as motor planning processes in the PMv and execution processes in the SMC (Taniwaki et al., 2003; 2006), age-related alteration in these functions might bring about not only decreased connectivity within the CC loop, but also the tendency toward increased variability in frequency.

Increased connectivity within motor cortices

Our SEM showed increased connectivity within motor cortices and between cerebral hemispheres. In SI tasks, moderate interactions were observed from the right SMA to the right SMC, from the right PMv to the right SMC, and the left PMv to right PMv in the aged subjects. Bilateral SMAs showed moderate positive reciprocal influences. The role of the SMA in behavior remains elusive, but many functions have been ascribed to this region including internal planning (Tanji and Shima, 1994), timing (Macar et al., 2004), sequencing (Shima and Tanji, 1998) and action retrieval (Chen et al., 1995). Our results from the ET tasks

showed that aged subjects have stronger interactions among the bilateral PMv, SMA and SMC, which reflect motor planning processes in the PMv and execution processes in the SMC. Since this connectivity in the aged group includes neither the basal ganglia nor the cerebellum, intercortical interactions might be strengthened for good motor performance.

Interhemispheric interactions were more obvious in aged subjects than in young subjects. It is possible that these interhemispheric interactions represent either transcallosal inhibition or facilitation. SEM results need to be interpreted carefully because of methodological limitations. We cannot always interpret a positive path coefficient as an excitatory influence and a negative path coefficient as inhibitory (McIntosh and Gonzalez-Lima, 1994). Instead, positive and negative path coefficients measure signs of covariance relationships among the structures of a network. Our finding of stronger interhemispheric interactions in aged subjects could be regarded as reflecting quantitative changes within a functional network that may be comparable to reduced functional lateralization in the aged motor cortex (Naccarato et al., 2006). These differences might be more related to the greater demands in aged subjects on maintaining and updating working memory, attending to multiple actions and/or response conflict monitoring.

Previous imaging studies have shown greater activation of motor cortices in elderly subjects, in both spatial extent and magnitude (Esposito et al., 1999; Grady, 2000; Hutchinson et al., 2002; Mattay et al., 2002; Wu and Hallett, 2005). A recent study using rTMS and PET reported enhanced local effective connectivity between motor-related areas in aged subjects (Rowe et al., 2006). Our current results also showed increased connectivity within motor cortices and between hemispheres. Several imaging studies of motor behavior provide support for the interpretation that greater activity is a compensatory response to increased functional demands (Hutchinson et al., 2002; Mattay et al., 2002; Wu and Hallett, 2005), although a recent study did not support this interpretation (Riecker et al., 2006). The increased interactions within motor cortices in our elderly subjects may also be a consequence of the reorganization and redistribution that takes place in brain circuitry in response to neurodegeneration (Mattay et al., 2002; Wu and Hallett, 2005). It is possible that increased connectivity within motor cortices is the product of a breakdown in local inhibitory processes, secondary to neural degeneration leading to intracortical disconnectivity (Mattay et al., 2002).

Concluding remarks

A combined use of sequential finger movements, fMRI and SEM enabled us to visualize the effects of age on functional connectivity within motor loops in the basal ganglia and cerebellum during motor execution. Different functional interactions within cortico-subcortical loops and intracortical loops were demonstrated. The functional changes that occur in the BGTM and CC loops in neurological disorders remain to be determined; analysis of patients with Parkinson's disease, currently progress in our laboratory, will help to address this question.

References

Alexander, G.E., Crutcher, M.D., Delong, M.R., 1990. Basal ganglia thalamo-cortical circuits: parallel substrates for motor, oculomotor, "prefrontal" and "limbic" functions. Prog. Brain Res. 85, 119–146.

Andersen, B.B., Gundersen, H.J.G., Pakkenberg, B., 2003. Aging of the human cerebellum: a stereological study. J. Comp. Neurol. 466, 356–365.

Barbas, H., Pandya, D.N., 1987. Architecture and frontal cortical connections of the premotor cortex (area 6) in the rhesus monkey. J. Comp. Neurol. 256, 211–228.

Bullmore, E., Horwitz, B., Honey, G., Brammer, M., Williams, S., Sharma, T., 2000. How good is good enough in path analysis of fMRI data? NeuroImage 11, 289–301.

Büchel, C., Wise, R.J.S., Mummery, C.J., Poline, J.-B., Friston, K.J., 1996. Nonlinear regression in parametric activation studies. NeuroImage 4, 60–66.

Büchel, C., Holmes, A.P., Rees, G., Friston, K.J., 1998. Characterizing stimulus–response functions using nonlinear regressors in parametric fMRI experiments. NeuroImage 8, 140–148.

Calautti, C., Serrati, C., Baron, J.C., 2001. Effects of age on brain activation during auditory-cued thumb-to-index opposition: a positron emission tomography study. Stroke 32, 139–146.

Casini, L., Ivry, R.B., 1999. Effects of divided attention on temporal processing in patients with lesions of the cerebellum or frontal lobe. Neuropsychology 13, 10–21.

Chen, Y.-C., Thaler, D., Nixon, P.D., Stern, C.E., Passingham, R.E., 1995. The functions of the medial premotor cortex (SMA) II. The timing and selection of learned movements. Exp. Brain Res. 102, 461–473.

Delong, M.R., 1990. Primate models of movement disorders of basal ganglia origin. Trends Neurosci. 13, 281–285.

Esposito, G., Kirkby, B.S., Van Horn, J.D., Ellmore, T.M., Berman, K.F., 1999. Context-dependent, neural system-specific neurophysiological concomitants of ageing: mapping PET correlates during cognitive activation. Brain 122, 963–979.

Fang, M., Li, J., Lu, G., Gang, X., Yew, D.T., 2005. A fMRI study of age-related differential cortical patterns during cued motor movement. Brain Topogr. 17, 127–137.

Friston, K.J., Holmes, A.P., Worsley, K.J., Poline, J.-P., Frith, C.D., Frackowiak, R.S., 1995. Statistical parametric maps in functional imaging: a general linear approach. Hum. Brain Mapp. 2, 189–210.

Friston, K.J., Holmes, A.P., Worsley, K.J., 1999. How many subjects constitute a study? NeuroImage 10, 1–5.

Grady, C.L., 2000. Functional brain imaging and age-related changes in cognition. Biol. Psychol. 54, 259–281.

Grafton, S.T., Sutton, J., Couldwell, W., Lew, M., Waters, C., 1994. Network analysis of motor system connectivity in Parkinson's disease: modulation of thalamocortical interactions after pallidotomy. Hum. Brain Mapp. 2, 45–55.

Hedden, T., Gabrieli, J.D., 2004. Insights into the ageing mind: a view from cognitive neuroscience. Nat. Rev., Neurosci. 5, 87–96.

Hutchinson, S., Kobayashi, M., Horkan, C.M., Pascual-Leone, A., Alexander, M.P., Schlaug, G., 2002. Age-related differences in movement representation. NeuroImage 17, 1720–1728.

Ivry, R.B., Keele, S.W., Diener, H.C., 1988. Dissociation of the lateral and medial cerebellum in movement timing and movement execution. Exp. Brain Res. 73, 167–180.

Jancke, L., Specht, K., Mirzazade, S., Peters, M., 1999. The effect of finger-movement speed of the dominant and subdominant hand on cerebellar activation: a functional magnetic resonance imaging study. NeuroImage 9, 497–507.

Johnson, P.B., Ferraina, S., Bianchi, L., Caminiti, R., 1996. Cortical networks for visual reaching: physiological and anatomical organization of frontal and parietal lobe arm regions. Cereb. Cortex 6, 102–119.

Kaasinen, V., Vilkman, H., Hietala, J., Nagren, K., Helenius, H., Olsson, H., Farde, L., 2000. Age-related dopamine D2/D3 receptor loss in extrastriatal regions of the human brain. Neurobiol. Aging 21, 683–688.

Kelly, R.M., Strick, P.L., 2003. Cerebellar loops with motor cortex and prefrontal cortex of a nonhuman primate. J. Neurosci. 23, 8432–8444.

Kondo, H., Morishita, M., Osaka, N., Osaka, M., Fukuyama, H., Shibasaki, H., 2004. Functional roles of the cingulo-frontal network in performance on working memory. NeuroImage 21, 2–14.

Laforce, R., Doyon, J., 2002. Differential role for the striatum and cerebellum in response to novel movements using motor learning paradigm. Neuropsychologia 40, 512–517.

Macar, F., Anton, J.L., Bonnet, M., Vidal, F., 2004. Timing functions of the supplementary motor area: an event-related fMRI study. Brain Res. Cogn. Brain Res. 21, 206–215.

Mann, D.M.A., Yates, P.O., 1979. The effects of ageing on the pigmented nerve cells of the human locus caeruleous and substantia nigra. Acta Neuropathol. 47, 93–97.

Mark, R.E., Rugg, M.D., 1998. Age effects on brain activity associated with episodic memory retrieval. An electrophysiological study. Brain 121, 861–873.

Mattay, V.S., Callicott, J.H., Bertolino, A., Santha, A.K.S., van Horn, J.D., Tallent, K.A., Frank, J.A., Weinberger, D.R., 1998. Hemispheric control of motor function: a whole brain echo planar fMRI study. Psychiatry Res. 83, 7–22.

Mattay, V.S., Fera, F., Tessitore, A., Hariri, A.R., Das, S., Callicott, J.H., Weinberger, D.R., 2002. Neurophysiological correlates of age-related changes in human motor function. Neurology 58, 630–635.

McIntosh, A.R., Gonzalez-Lima, F., 1994. Structural equation modeling and its application to network analysis in functional brain imaging. Hum. Brain Mapp. 2, 2–22.

McIntosh, A.R., Grady, C.L., Ungerleider, L.G., Haxby, J.V., Rapoport, S.I., Horwitz, B., 1994. Network analysis of cortical visual pathways mapped with PET. J. Neurosci. 14, 655–666.

Middleton, F.A., Strick, P.L., 2000. Basal ganglia and cerebellar loops: motor and cognitive circuits. Brain Res. Rev. 31, 236–250.

Muakkassa, K.F., Strick, P.L., 1979. Frontal lobe inputs to primate motor cortex: evidence for four somatotopically organized 'premotor areas'. Brain Res. 177, 176–182.

Naccarato, M., Calautti, C., Jones, P.S., Day, D.J., Carpenter, T.A., Baron, J.-C., 2006. Does healthy aging affect the hemispheric activation balance during paced index-to-thumb opposition task? An fMRI study. NeuroImage 32, 1250–1256.

O'Boyle, D.J., Freeman, J.S., Cody, F.W.J., 1996. The accuracy and precision of timing of self-paced, repetitive movements in subjects with Parkinson's disease. Brain 119, 51–70.

Oldfield, R.C., 1971. The assessment and analysis of handedness: the Edinburgh inventory. Neuropsychologia 9, 97–113.

Park, H.L., O'Connell, J.E., Thomson, R.G., 2003. A systematic review of cognitive decline in the general elderly population. Int. J. Geriatr. Psychiatry 18, 1121–1134.

Pastor, M.A., Jahanshahi, M., Artieda, J., Obeso, J.A., 1992. Performance of repetitive wrist movements in Parkinson's disease. Brain 115, 875–891.

Pastor, M.A., Day, B.L., Macaluso, E., Friston, K.J., Frackowiak, R.S.J., 2004. The functional neuroanatomy of temporal discrimination. J. Neurosci. 24, 2585–2591.

Riecker, A., Groschel, K., Ackermann, H., Steinbrink, C., Witte, O., Kastrup, A., 2006. Functional significance of age-related differences in motor activation patterns. NeuroImage 32, 1345–1354.

Rizzolatti, G., Luppino, G., Matelli, M., 1998. The organization of the cortical motor system: new concepts. Electroencephalogr. Clin. Neurophysiol. 106, 283–296.

Rouiller, E.M., Babalian, A., Kazennikov, O., Moret, V., Yu, X.M., Wiesendanger, M., 1994. Transcallosal connections of the distal forelimb representations of the primary and supplementary motor cortical areas in macaque monkeys. Exp. Brain Res. 102, 227–243.

Rowe, J., Stephan, K.E., Friston, K., Frackowiak, R.S., Lees, A., Passingham, R., 2002. Attention to action in Parkinson's disease: impaired effective connectivity among frontal cortical regions. Brain 125, 276–289.

Rowe, J.B., Siebner, H., Filipovic, S.R., Cordivari, C., Gerschlager, W., Rothwell, J., Frackowiak, R., 2006. Aging is associated with contrasting changes in local and distant cortical connectivity in the human motor system. NeuroImage 32, 747–760.

Sailer, A., Dichgans, J., Gerloff, C., 2000. The influence of normal aging on the cortical processing of a simple motor task. Neurology 55, 979–985.

Shima, K., Tanji, J., 1998. Both supplementary and presupplementary motor areas are crucial for the temporal organization of multiple movements. J. Neurophysiol. 80, 3247–3260.

Smith, C.D., Umberger, G.H., Manning, E.L., Slevin, J.T., Wekstein, D.R., Schmitt, F.A., Markesbery, W.R., Zhang, Z., Gerhardt, G.A., Kryscio, R.J., Gash, D.M., 1999. Critical decline in fine motor hand movements in human aging. Neurology 53, 1458–1461.

Taniwaki, T., Okayama, A., Yoshiura, T., Nakamura, Y., Goto, Y., Kira, J., Tobimatsu, S., 2003. Reappraisal of the motor role of basal ganglia: a functional magnetic resonance image study. J. Neurosci. 23, 3432–3438.

Taniwaki, T., Okayama, A., Yoshiura, T., Togao, O., Nakamura, Y., Yamasaki, T., Ogata, K., Shigeto, K., Ohyagi, Y., Kira, J., Tobimatsu, S., 2006. Functional network of the basal ganglia and cerebellar motor loops in vivo: different activation patterns between self-initiated and externally triggered movements. NeuroImage 31, 745–753.

Tanji, J., Shima, K., 1994. Role of supplementary motor area cells in planning several movements ahead. Nature 371, 413–416.

Vakil, E., Kahan, S., Huberman, M., Osimani, A., 2000. Motor and non-motor sequence learning in patients with basal ganglia lesions: the case of serial reaction time (SRT). Neuropsychologia 38, 1–10.

Volkow, N.D., Gur, R.C., Wang, G.J., Fowler, J.S., Moberg, P.J., Ding, Y.S., Hitzemann, R., Smith, G., Logan, J., 1998. Association between decline in brain dopamine activity with age and cognitive and motor impairment in healthy individuals. Am. J. Psychiatry 155, 344–349.

Ward, N.S., Frackowiak, R.S.J., 2003. Age-related changes in the neural correlates of motor performance. Brain 126, 873–888.

Welford, A.T., 1988. Reaction time, speed of performance, and age. Ann. N. Y. Acad. Sci. 515, 1–17.

Wu, T., Hallett, M., 2005. The influence of normal human ageing on automatic movements. J. Physiol. 562, 605–615.

Available online at www.sciencedirect.com
ScienceDirect
Neurochemistry International 51 (2007) 227–232
NEUROCHEMISTRY International
www.elsevier.com/locate/neuint

A neurotoxic dose of methamphetamine induces gene expression of Homer 1a, but not Homer 1b or 1c, in the striatum and nucleus accumbens

Kijiro Hashimoto [a], Tatsuo Nakahara [a], Hidetaka Yamada [a], Makoto Hirano [a], Toshihide Kuroki [a,b,*], Shigenobu Kanba [b]

[a] *Center for Emotional and Behavioral Disorder, National Hospital Organization Hizen Psychiatric Center, Kanzaki, Saga 842-0192, Japan*
[b] *Department of Neuropsychiatry, Kyushu University Graduate School of Medical Sciences, Fukuoka 812-8582, Japan*

Received 5 April 2007; received in revised form 17 May 2007; accepted 22 May 2007
Available online 8 June 2007

Abstract

Homer proteins, which regulate the signaling pathway of metabotropic glutamate receptors, may contribute to the glutamatergic modulation of dopamine neurons in the basal ganglia. This study examined whether the induction of Homer 1 genes is or not associated with the methamphetamine-induced dopaminergic neurotoxicity in the discrete brain regions of rats. Basal levels of Homer 1a and 1c mRNAs in the forebrain regions were higher than those in the substantia nigra, whereas Homer 1b mRNA levels were higher in the substantia nigra than those in the forebrain regions examined. A neurotoxic dose (40 mg/kg, i.p.) of methamphetamine increased the mRNA and protein levels of Homer 1a in the striatum and nucleus accumbens, but not in the medial prefrontal cortex or the substantia nigra. Both Homer 1b and 1c mRNAs were not affected in any brain regions examined. These results suggest that the induction of Homer 1a gene may be involved at least in part in the methamphetamine-induced dopaminergic neurotoxicity, possibly through the glutamate-dopaminergic interaction.

Keywords: Homer; Methamphetamine; Neurotoxicity; Striatum; Nucleus accumbens

1. Introduction

The interactions between dopamine and glutamate within the various brain regions including the basal ganglia have significant implications for the pathophysiology of schizophrenia and Parkinson's disease (Carlsson and Carlsson, 1990). Many lines of evidence (Morari et al., 1998; Vandershuren and Kalivas, 2000) suggest the glutamatergic control of dopamine transmission and vice versa in the striatum, nucleus accumbens and prefrontal cortex.

Homer proteins have found to be involved in the molecular mechanism for the signaling pathway of metabotropic glutamate receptors (mGluRs) (Brakeman et al., 1997; Kato et al., 1997). The Homer family consists of three independent genes such as Homer 1, 2 and 3. Moreover, Homer 1 comprises three splicing variants; Homer 1a, 1b, and 1c (Xiao et al., 1998). Homer 1a is an immediate early gene (IEG) product that is rapidly responsive to neuronal activity (Brakeman et al., 1997; Kato et al., 1997; Berke et al., 1998), while other members of the Homer family are constitutively expressed. Seizure is reported to induce Homer 1a dramatically in the hippocampus (Brakeman et al., 1997; Xiao et al., 1998; Kato et al., 1998; Morioka et al., 2001; Bottai et al., 2002), striatum and cortex (Kato et al., 1998), and light stimuli also induced it in the suprachiasmatic nuclei (Brakeman et al., 1997; Park et al., 1997; Nielsen et al., 2002). Recently, dopaminergic modulation has been demonstrated to affect gene expression of Homer 1a. Cocaine, a dopamine transporter inhibitor (Brakeman et al., 1997; Swanson et al., 2001), SKF38393, a D_1 receptor agonist (Berke et al., 1998; Yamada et al., 2007), and haloperidol, a D_2 receptor antagonist (de Bartolomeis et al., 2002; Polese et al., 2002), induced the Homer 1a gene expression in the striatum. In

* Corresponding author at: Department of Neuropsychiatry, Kyushu University Graduate School of Medical Sciences, Fukuoka 812-8582, Japan. Tel.: +81 92 642 5621; fax: +81 92 642 5644.
E-mail address: toshik@npsych.med.kyushu-u.ac.jp (T. Kuroki).

0197-0186/$ – see front matter © 2007 Elsevier Ltd. All rights reserved.
doi:10.1016/j.neuint.2007.05.017

contrast, SCH23390, a D_1 receptor antagonist, attenuated methylphenidate-induced expression of striatal Homer 1a (Yano et al., 2006). Moreover, Homer 1b- and 1c-knockout mice displayed enhanced methamphetamine-induced motor behavior (Szumlinski et al., 2005), while behavioral response to amphetamine increased in transgenic mice overexpressing Homer 1a in striatal medium spiny neurons localized predominantly in the striosome (patch) (Tappe and Kuner, 2006). These findings suggest that Homer 1a could play a key role on dopamine–glutamate interactions in the striatum.

Administration of high doses (more than 20 mg/kg) of methamphetamine is known to cause the neurotoxic effect on dopamine terminals in the striatum and nucleus accumbens of rodent brain (Fukumura et al., 1998), as indicated by degenerative changes in microscopic morphology, depletion of tissue dopamine contents, decreases in enzymatic activity of dopamine synthesis and number of dopamine transporters (Seiden and Ricaurte, 1987). Methamphetamine-induced increases in extracellular levels of dopamine as well as glutamate may contribute to oxidative stress and/or excitoxicity that damage dopamine neurons (Nash and Yamamoto, 1993; Xue et al., 1996). Because of a possible involvement of Homer 1a in the dopamine-glutamate interaction, the induction of this protein may be associated with methamphetamine-induced dopaminergic neurotoxicity.

To test this hypothesis, we examined the effect of a neurotoxic dose of methamphetamine on gene expression of Homer 1 in the discrete brain regions of rats.

2. Methods

2.1. Animals

Male Wistar rats (Kyudo Animal Laboratory, Kumamoto, Japan) weighing 220–240 g were housed four per cage, maintained on a 12 h light/12 h dark cycle and given access to food and water *ad libitum*. All procedures were done in accordance with Principles of Laboratory Animal Care (NIH publication no. 86-23, revised 1985).

2.2. Drug treatment

Methamphetamine (Dainippon Pharmaceutical Co., Osaka, Japan) was dissolved in 0.9% NaCl and injected intraperitoneally (i.p.) in a volume of 1 ml/kg body weight. For analysis of Homer mRNAs, rats were given methamphetamine (40 mg/kg, i.p.) 1, 2 and 4 h prior to sacrifice ($n = 9$ for each time point). Control group of rats received saline 1 h prior to sacrifice ($n = 9$). For Western blot assays of Homer 1a, the animals were injected with methamphetamine (40 mg/kg) ($n = 10$) or saline ($n = 10$), and then killed 4 h after the injections. The dose of methamphetamine (40 mg/kg) was chosen on the basis of the methamphetamine-induced neurotoxicity to produce long-lasting depletion of contents, synthesis rate and transporter numbers of dopamine (Fukumura et al., 1998; Seiden and Ricaurte, 1987). This dose of methamphetamine was also employed in the previous study (Nakahara et al., 2003; Thiriet et al., 2001) demonstrating the time-dependent profile of the IEG c-fos mRNA levels, together with that of tissue contents of dopamine, serotonin and their metabolites following methamphetamine administration.

2.3. Tissue preparation

The brain was quickly removed and stored at −80 °C. Serial slices of 300 μm were made from the removed brain in a cryostat at −12 °C, and four brain regions were dissected freehand with a microknife, as described previously (Nakahara et al., 1990). Total RNA was prepared from the brain tissue by the method of Chomczynski and Sacchi (1987).

2.4. Reverse transcription-polymerase chain reaction (RT-PCR)

The levels of mRNAs in the discrete brain regions were quantified by reverse transcription-polymerase chain reaction (RT-PCR) with an endogenous internal standard, β-actin, as previously described (Gotoh et al., 2002; Nakahara et al., 2005; Yamada et al., 2007). RT was performed on 1 μg total RNA for 90 min at 42 °C in a 5 μl reaction mixture containing 25 mM Tris-HCl (pH 8.3), 50 mM KCl, 5 mM $MgCl_2$, 2 mM dithiothreitol, 1 mM each deoxynucleotide, 10 U AMV reverse transcriptase (Roche Molecular Biochemicals, Mannheim, Germany), 10 U rebonuclease inhibitor (Roche Molecular Biochemicals) and 0.8 μg oligo $(dT)_{15}$ primer (Roche Molecular Biochemicals). The RT was terminated by heating the sample at 95 °C for 2 min. The multiplexed PCR was carried out in a 20 μl reaction mixture containing 10 mM Tris-HCl (pH 8.3), 50 mM KCl, 1.5 mM $MgCl_2$, 2% dimethyl sulfoxide, 0.2 mM each deoxynucleotide, 0.1 μM each of 5′ and 3′ β-actin-specific primers, 1 μM each of 5′ and 3′ specific primers, 25 ng of reverse-transcribed total RNA, and 0.5 U Taq DNA polymerase (Roche Molecular Biochemicals). The PCR primers used for amplification of β-actin and Homer mRNAs were as follows (GenBank accession number): β-actin (V01217), 5′-TCATGCCATCCTGCGTCTGGACCT-3′ (forward); 5′-CCGGACTCATCGTACTCCTGCTTG-3′ (reverse); target sequence = 582 bp; Homer 1a (AJ276327), 5′-TGGACTGGGATTCTCCTCTG-3′ (forward); 5′-CCATCTCATTTAATCATGATTGC-3′ (reverse); target sequence = 309 bp; Homer 1b (AF093267), 5′-CCAGTACCCCTTCACAGGAA-3′ (forward); 5′-TGCTTCACGTTGGCAGTG-3′(reverse); target sequence = 259 bp; Homer 1c (AF093268), 5′-CCAGTACCCCTTCACAGGAA-3′ (forward); 5′-TGCTTCACGTTGGCAGTG-3′ (reverse); target sequence = 295 bp. The PCR amplification was performed for 28 cycles, consisting of denaturation (94 °C, 45 s), annealing (60 °C, 45 s), and extension (72 °C, 75 s). After six cycles, 0.1 μM each of β-actin primer pair was added to the reaction mixture and PCR cycles were further continued.

The PCR products were analyzed on a 10% polyacrylamide gel electrophoresis. Gels were stained with ethidium bromide, visualized with UV transillumination, photographed, and submitted to image analysis. Quantitative image analysis of the PCR fragments was performed using the NIH image program. The levels of mRNAs were calculated as the ratios of optical density of each PCR product to that of the β-actin PCR product.

2.5. Western blot of Homer 1a

The striatal tissues were lysed by sonication (10%, 15 s; Ultrasonic Cell Disruptor, Heat System-Ultorasonics, Farmingdale, NY) in 10 volumes of the lysis buffer (20 mM Tris–HCl, pH 7.4, 1 mM EDTA and 1% Triton X-100) and centrifuged at 13,000 × *g* for 30 min at 4 °C, and then the supernatant was collected. The protein concentration of supernatant was determined using the Bradford colorimetric assay (Wako, Pure Chemical Industries Ltd., Osaka, Japan) following manufacturer's instructions. The supernatants were mixed with an equal volume of 2× SDS gel-loading buffer (125 mM Tris–HCl, pH 6.8, 100 mM dithiothreitol, 4% SDS, 0.2% bromophenol blue and 20% glycerol) and then boiled for 5 min. Aliquots of protein (100 μg/lane) were separated by sodium dodecyl sulfate-polyacrylammide gel electrophoresis (SDS-PAGE) containing 12% polyacrylamide. Separated proteins were transferred to PVDF (polyvinylidenedifluoride) membranes (Roche, Mannheim, Germany) using an electrophoretic transfer kit (LKB, Uppsala, Sweden). Nonspecific sites on the PVDF membrane were blocked by incubating in 5% nonfat dried milk (Amersham, Buckinghamshire, UK) in TBST (20 mM Tris–HCl, pH 7.6, 137 mM NaCl, 0.1% Tween-20) for 1 h. The membranes were incubated with a goat anti-Homer 1a polyclonal antibody (1:1000; Santa Cruz Biotechnology, Santa Cruz, CA) for 1 h at room temperature. After washing in TBST, the membranes were incubated in the anti-goat secondary antibody conjugated to horseradish peroxidase (1:3000; R&D System, Minneapolis, MN) for 1 h at room temperature. Immunoblots were washed with TBST, incubated in ECL solution (Amersham) and apposed to film (Hyperfilm, Amersham). The intensity of the visualized immunoreactive protein was quantified using NIH Image software.